POLITECNICO DI TORINO
Repository ISTITUZIONALE

A modular system identification approach to spread mooring dynamics: Numerical and experimental case studies

Original
A modular system identification approach to spread mooring dynamics: Numerical and experimental case studies / Paduano, B., Niosi, F., Dell'Edera, O., Issoglio, D., Dutto, L., Faedo, N.. - In: APPLIED OCEAN RESEARCH. - ISSN 0141-1187. - 175:(2026), p. 105205. [10.1016/j.apor.2026.105205]

Availability:
This version is available at: 11583/3016634 since: 2026-10-14T09:07:21Z

Publisher:
Elsevier

Published
DOI:10.1016/j.apor.2026.105205

Terms of use:

This article is made available under terms and conditions as specified in the corresponding bibliographic description in the repository

Publisher copyright

(Article begins on next page)

19 November 2026

Applied Ocean Research 175 (2026) 105205



Contents lists available at ScienceDirect

Applied Ocean Research

journal homepage: www.elsevier.com/locate/apor



Research paper



A modular system identification approach to spread mooring dynamics: Numerical and experimental case studies

Bruno Paduano *, Francesco Niosi, Oronzo Dell'Edera, Davide Issoglio, Lorenzo Dutto, Nicolás Faedo

Marine Offshore Renewable Energy Lab, Politecnico di Torino, Corso Duca degli Abruzzi, 24, Turin 10121, Piedmont, Italy

ARTICLE INFO

Keywords:
Mooring systems
System identification
Floating offshore wind
Wave energy converters
Experimental validation

ABSTRACT

Numerical simulation of mooring dynamics is computationally expensive, which limits its use in optimisation and control loops; data-driven system identification (SI) offers a complementary route. This work reviews the state-of-the-art of SI for mooring modelling and proposes a modular framework in which the empirical transfer function of a single mooring line is identified in the frequency domain and used, via a coordinate change, to reconstruct the global response of spread taut and semi-taut mooring configurations. The framework is assessed on a numerical wave energy converter benchmark and validated experimentally on a 1:96 reduced-scale floating offshore wind turbine with a taut-leg mooring. The identified models reproduce the dominant mooring dynamics at a fraction of the computational cost of finite-element simulations and recover physically meaningful line properties; limitations under catenary, slack-line and extreme-state regimes are explicitly discussed.

1. Introduction

Mooring systems play a fundamental role in the dynamics of floating structures. While their primary objective is to restrain motions and ensure floater survivability, the wide range of applications and the intricate complexity of station-keeping systems necessitate a more detailed analysis regarding the influence of mooring configurations in the overall response of any given marine structure. Mooring designs vary significantly across different applications, ranging from floating production storage and offloading (FPSO) units (Ja'e et al., 2022a), to novel wave energy converters (WECs) (Ja'e et al., 2022b), and floating offshore wind turbine (FOWT) systems (Brommundt et al., 2012). Beyond the single-body configurations recalled above, an increasing number of emerging offshore applications rely on multi-module or interconnected floating structures, where the mooring problem cannot be reduced to a single-body analysis. Representative examples include modular three-module semi-submersible platforms, for which dedicated mooring layouts must be designed to accommodate the inter-module hydrodynamic coupling (Yu et al., 2024); wind-aquaculture hybrid platforms, whose fully-coupled response involves strong interactions between hydrodynamics, mooring lines, and integrated subsystems (Huang et al., 2026); and multi-module floating photovoltaic arrays, in which the mooring design must additionally account for tidal variations and the composite nature of the lines (Tang et al., 2024). In these systems, the mooring dynamics is further complicated by the load-sharing between connectors and mooring lines, and by the potentially cascading consequences of connector or line failures on the overall system safety (Cai et al., 2026). A comprehensive overview of the recent developments in the modelling and design of mooring systems for such multi-module structures is provided by the recent review by Saincher et al. (2025).

The primary objective of mooring systems remains anchored in ensuring the survivability of the floater. To achieve suitable configurations, mooring designers must often contend with a complex and computationally expensive simulation framework. This framework is generally mandated by standards and required for certification purposes (DNV, 2015; IEC, 2019), requiring an analysis across a broad range of conditions. This includes both extreme and damaged conditions (Subbulakshmi and Verma, 2024), as well as a fatigue assessment (Aursand et al., 2023) for moorings designed to last over five years. The standard approach can be extremely time-consuming and typically involves extensive nonlinear simulations, relying on a statistical methodology based on extreme value distributions (Fraga and Neves, 2011). Additionally, mooring design must consider several extra constraints, such as ensuring the safety of the umbilical cables that guarantee electric energy transmission (Ullah and Choi, 2024), and limiting the motion of the floater to reduce fatigue damage, particularly in FOWTs (Bradshaw et al., 2024). These constraints can be integrated

* Corresponding author.
E-mail address: bruno.paduano@polito.it (B. Paduano).

https://doi.org/10.1016/j.apor.2026.105205
Received 31 March 2026; Received in revised form 1 July 2026; Accepted 4 August 2026
Available online 20 August 2026
0141-1187/© 2026 The Authors. Published by Elsevier Ltd. This is an open access article under the CC BY license (http://creativecommons.org/licenses/by/4.0/).

List of abbreviations

ARX	autoregressive exogenous
BEM	boundary element method
CALM	catenary anchor leg mooring
CFD	computational fluid dynamics
CoM	centre of mass
EMD	empirical mode decomposition
ETFE	empirical transfer function estimate
FoR	frame of reference
FOWT	floating offshore wind turbine
FPSO	floating production storage and offloading
I/O	input/output
MIMO	multiple-input-multiple-output
NARX	nonlinear autoregressive exogenous
NN	neural network
NRMSA	normalised root mean squared accuracy
NWT	numerical wave tank
ROV	remote operating vehicle
SI	system identification
SISO	single-input-single-output
SPM	single point mooring
STFT	short-time Fourier transform
TLP	tension leg platform
WEC	wave energy converter

into a general mooring design problem, which can be informally posed as follows:

$$\Sigma : \begin{cases} \min(\mathcal{F}_{\text{cost}}), \\ \text{subject to:} \\ \text{floater survivability}, \\ \text{components safety}, \\ \text{system working principle}, \end{cases} \tag{1}$$

where the mooring design problem Σ is defined as the minimisation of an economic function $\mathcal{F}_{\text{cost}}$, while ensuring floater survivability, safety of the involved components, and a proper functioning of the system. A significantly more complex analysis is required for WECs, where the working principle is generally linked to power maximisation through motion maximisation (due to the resonant nature of WECs) (Carapellese et al., 2023) and, clearly, mooring systems can significantly influence such objective (Papini et al., 2023; Paduano et al., 2024).

From the discussion provided above, and the intrinsic requirements involved in mooring design, the following main research question can be posed: *how can the mooring response be predicted and analysed efficiently using numerical models*? While standards suggest that static or quasi-static approaches may be sufficient for some cases (DNV, 2015), typically, mooring systems are analysed using numerical dynamic modelling techniques. These techniques often employ finite-difference methods (Hall and Goupee, 2015; Hall, 2020) or finite-element discretisation (Palm, 2017), driven by the need to account for relevant nonlinear phenomena, including *e.g.* seabed interaction, asymmetrical line response, friction, damping, and hysteresis, among others (Tsukrov et al., 2005; Ma et al., 2019). It is indeed true that the broad range of simulations required to analyse the significant aspects of mooring dynamics, and their influence on the floater response, makes the nonlinear, time-consuming simulations, necessary to accurately represent mooring dynamics, a substantial limitation. Consequently, research is increasingly focusing on developing novel modelling approaches to address the mooring problem, advancing towards mooring optimisation techniques (Peña-Sanchez et al., 2024; Ja'e et al., 2022a), and including mooring dynamics in control problems (Bruno Paduano et al., 2023), recognising their influence in the overall dynamics of any given floating structure. These modern modelling techniques typically rely on data, and leverage system identification (SI) methods to generate representative models. The application of such methods marks an interesting evolution in the state-of-the-art of mooring modelling, as they are capable of reducing simulation times by various orders of magnitude. Yet, *how do these methods work, and what is the current status of their application in mooring systems?*

Given the need to both critically assess existing mooring modelling approaches and to advance towards more efficient and interpretable frameworks, this study pursues the following objectives:

- to review the state-of-the-art in mooring system modelling, with particular emphasis on data-driven and SI techniques and their current level of adoption in mooring dynamics;
- to develop a general modelling framework tailored to spread mooring systems, which represent the most widely adopted configuration in offshore applications;
- to extensively assess the proposed approach using a numerical benchmark based on a WEC, selected for its pronounced dynamic response and suitability for systematic identification studies;
- to demonstrate the applicability of the methodology in a realistic setting by validating it against experimental data obtained from a reduced-scale FOWT.

By combining two reference case studies, one purely numerical and one experimental, this work illustrates how relatively simple and intuitive identification techniques can be effectively employed to predict mooring system behaviour and to infer key mooring line characteristics. Particular emphasis is placed on maintaining a strong link between the identified models and their underlying physical interpretation, thereby promoting physics-informed identification strategies suitable for both analysis and design-oriented applications.

The framework proposed in this study differs from the prior data-driven and SI-related works summarised in Table 1 primarily in its modular architecture: the global mooring response is reconstructed from the identification of a single mooring line, via a change of coordinates imposed by the spread layout. This modularity is, in our view, the central methodological contribution of the paper, and is what most distinguishes it from prior approaches, which typically formulate identification as a monolithic problem on either the whole mooring system or the closed-loop moored device. A direct consequence of this architecture is that the identification of the single line can be addressed independently of the global problem, and is therefore agnostic with respect to the specific identification technique adopted, whether linear or nonlinear, and whether parametric or non-parametric. In the present manuscript we adopt a frequency-domain formulation, based on an empirical transfer function estimate (ETFE), which is shown to be appropriate for the spread taut and semi-taut mooring layouts considered. The combination of the modular architecture and the frequency-domain identification yields a description that is straightforward, intuitive, and physically interpretable: the identified transfer function retains a direct correspondence with the underlying line stiffness. Possible extensions of the same modular framework to nonlinear identification structures, suitable for catenary or hybrid mooring configurations, are discussed in Section 6.

The remainder of this study is organised as follows: Section 2 discusses the fundamentals of SI techniques and analyses the state-of-the-art. Section 3 defines the proposed modelling framework for mooring identification. Section 4 applies the proposed methodology and discusses the results. Section 5 apply the ID procedure to the experimental FOWT system. Section 6 remarks the limitation of the proposed modelling technique. Finally, conclusions are outlined in Section 7.

Notation

A generic target system will be denoted as $g(u)$, with its associated response y. In contrast, the identified system and data will be denoted as $\tilde{g}(\tilde{u})$, with the associated response $\tilde{y}$. Given a signal $q(t)$, the associated Fourier transform $\mathcal{F}(q(t))(j\omega)$ is indicated with the capital letter,

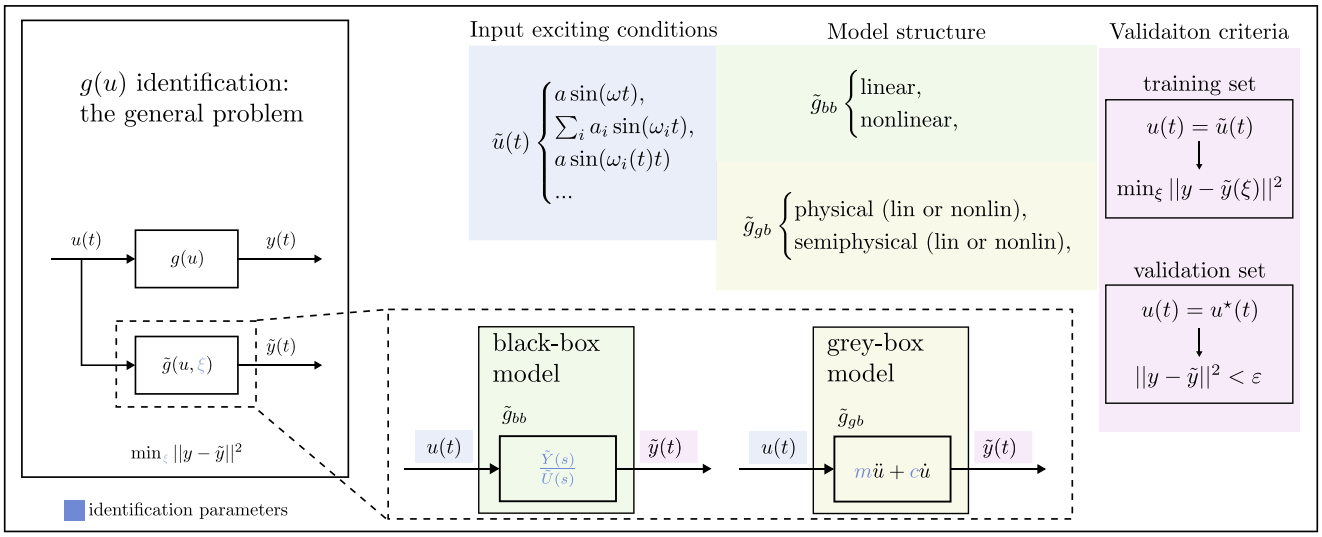


Fig. 1. Identification from data of a nonlinear system: a schematic representation. Please note that, $\tilde{g}_{bb}$, $\tilde{g}_{gb}$ refer to black-box and grey-box models, respectively.

i.e. $\mathcal{F}(q(t))(\jmath\omega) \equiv Q(\jmath\omega)$. With the exception of the wave elevation η, with its Fourier transform denoted as $\hat{\eta}$. Given $z \in \mathbb{C}$, the notation z^* is used to denote its complex-conjugate.

2. Mooring modelling approaches - state-of-the-art

Recent research has focused on novel, efficient approaches, driven by the increasing complexity of mooring design and the need for fast, accurate numerical methods. As the challenges in the mooring design field illuminate the need for new numerical tools, ranging from the derivation of computationally efficient and representative mooring responses, to innovative damage-detection methods, the state-of-the-art reveals an increasingly substantial utilisation of data-based and data-driven approaches. For instance, Pasta et al. (2023) provide an exhaustive overview of data-based and data-driven techniques for marine energy converters, with a focus on control-oriented approaches.

These methods form the primary framework for SI procedures. Therefore, to ensure this study remains reasonably self-contained, an overview of the SI techniques is provided prior to expanding on into the state-of-the-art.

Before proceeding, we wish to clarify the role and scope of the literature review presented in this section. The review is not intended to provide an exhaustive overview of mooring modelling and identification techniques, nor of mooring engineering as a whole; its purpose is to contextualise the proposed identification framework within the relevant state of the art, by highlighting the trends and the methodological gaps that motivate the contribution of this manuscript. The interested reader is referred to the recent review by Jiang (2025) for a comprehensive engineering overview of mooring system design, and to the standard references on system identification (e.g. Ljung and Glover (1981), Schoukens and Ljung (2019), Pintelon and Schoukens (2012)) for a complete treatment of the underlying methodology.

2.1. System identification - general framework

The main goal of SI is to find a representative *approximation* of the target system response, in terms of a mathematical model. It is important to understand that, while a model can provide a faithful description of a given phenomenon, there is inevitably some loss of data due to the underlying approximation. While the response for a known model can be straightforwardly evaluated, SI techniques aim to derive a representative model of a physical phenomenon, based on data available from the process. In a general framework, models can be classified as follows (Ljung, 1998):

- *White-box models:* the model is fully described in terms of its structure and parameters.
- *Grey-box models:* the model provides some insight into the physical phenomena, but some parameters still need to be determined.
- *Black-box models:* the model does not rely on the physical understanding of the phenomena.

Although white-box modelling does not require SI, the latter two model types are commonly used in various scenarios. This section briefly describes the foundations of SI techniques, particularly when dealing with nonlinear models, since the mooring response is intrinsically nonlinear.

Within a general framework, we consider an unknown process defined as:

$$y(t) = g(t, u, d), \tag{2}$$

where $y(t)$ represents the real output data of a given system $g(t, u, d)$, which is a function of a given exciting condition $u(t)$ and a disturbance $d(t)$. SI aims to find a model:

$$\tilde{y}(t) = \tilde{g}(t, \tilde{u}, \xi), \tag{3}$$

in which $\tilde{g}$ is parametrised by ξ to minimise, virtually always, the function $\|y - \tilde{y}\|^2$. Therefore, in aiming to evaluate the best approximation, which can be either linear[1] or nonlinear, a basic distinction in the identification process can be made based on whether it leverages a frequency-domain or time-domain description of the system g (Ljung and Glover, 1981).

If the designer chooses to represent the model in a non-parametric form (*i.e.*, frequency-domain), the identification process depends on defining the so-called best linear approximation (or even an empirical transfer function estimate) of a given system by approximating the target frequency response (Pintelon and Schoukens, 2012). Conversely, in the case of nonlinear models, a designer may adopt a time-varying structure by leveraging techniques such as the short-term Fourier transform (Allen, 1977) or nonlinear frequency response methods, for instance, using Volterra series approximation (Zhao et al., 2023; Prawin and Rao, 2017). Moreover, when nonlinear modelling techniques are required, it is more common to adopt a time-domain description of the system. In this context, we can still define linear models when the model structure is linear (*i.e.*, *linear in the parameters*

[1] While some models can be *locally* linear, the term "linear models" in this context is intended to describe a linear time-invariant system.

ξ) in Eq. (3). A straightforward example is the autoregressive model (Simpkins, 2012). Additionally, for nonlinear structures, models can be identified using techniques such as nonlinear autoregressors or neural networks (Schoukens and Ljung, 2019), among other methods.

A schematic and illustrative representation of the identification problem for a nonlinear system is depicted in Fig. 1, showing diverse examples of structures and input conditions. While the general identification procedure is described on the right-hand side of the figure and presented as a common least squares optimisation problem, the identification problem can be divided into three main components:

- *Input exciting conditions:* for model identification, the designer seeks to determine the input exciting conditions such that they can *represent* any further exciting conditions.
- *Model structure:* Defining the model structure is a critical aspect of the identification problem for a nonlinear system. Knowledge of the physical phenomena underlying the model plays a fundamental role in determining the structure of the candidate model.
- *Validation criteria:* While the SI problem can be defined to minimise the error function in the parameters ξ, model performance must be compared against a representative set of input conditions $u^\star(t) \neq \tilde{u}(t)$.

While the application of SI techniques to mooring analysis represents a relatively novel direction, the SI field has experienced significant growth over the past decades, and several references in this domain ground the methodology adopted in the present work. The frequency-domain identification approach used here, including the empirical transfer function description, follows the classical treatment of Ljung and Glover (1981) and the more recent textbook of Pintelon and Schoukens (2012). The general framework for the identification of nonlinear systems, which is the relevant reference for the possible extensions of the modular approach to catenary or hybrid mooring configurations discussed in Section 6, is comprehensively presented in Schoukens and Ljung (2019). The black-box and grey-box classification adopted throughout this work is built on Sjöberg et al. (1995), whereas Simpkins (2012) and Ljung (2010) are recommended as broader introductions to, and historical perspectives on, the field of system identification.

2.2. Towards innovative mooring modelling techniques - state-of-the-art

Within this section, an overview of the current techniques for modelling mooring systems (or moored systems) is provided. The reader will observe that the field is increasingly moving towards the development of computationally efficient numerical techniques, computationally efficient while retaining sufficient accuracy with respect to the reference model and consistency with available data. A general framework for a moored system is described in Fig. 2.

The floating body, responsible for wave interactions, is denoted as $g_d(\eta, f_m)$, and is subject to a generic environmental-induced disturbance field[2] η and the feedback reaction f_m, of the mooring system $g_m(x, \eta)$. In this generic framework, the mooring is described as a feedback system of the floater, acted upon by the system kinematics x, while being disturbed by the wave field η.[3] Studies in the state-of-the-art are categorised, according to Fig. 2, into three types:

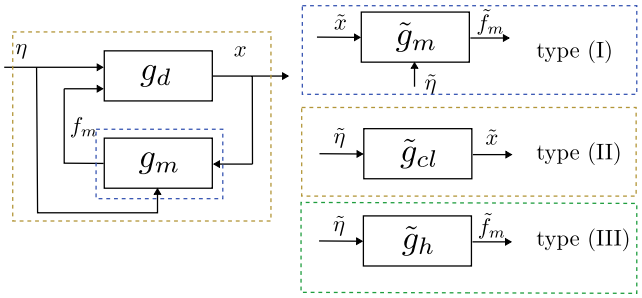


Fig. 2. General description of a moored system. Left: target system, with g_d the floater/wave interaction and g_m the mooring system. Right: classification of identified models.

- *Type (I)*: here, the only mooring system g_m is identified (achieving the associated approximated model $\tilde{g}_m$) by imposing the floater kinematics ($\tilde{u} = \tilde{x}$) and achieving an approximation of the mooring restoring force ($\tilde{y} = \tilde{f}_m$).
- *Type (II)*: in this case, the entire closed-loop system is identified (*i.e.* $\tilde{g}_{cl}$) by imposing a representative set of wave exciting conditions ($\tilde{u} = \tilde{\eta}$) and analysing the system response in terms of the kinematics of the moored device ($\tilde{y} = \tilde{x}$).
- *Type (III)*: this scenario involves a combination of Type (I) and Type (II), where the hybrid system ($\tilde{g}_h$) can be modelled as $\tilde{g}_h = \tilde{g}_{cl}\tilde{g}_m$, with the system input being the wave field ($\tilde{u} = \tilde{\eta}$) and the response characterised as the mooring restoring force ($\tilde{y} = \tilde{f}_m$).

To complete the classification of studies in literature a *Type (IV)* is added, gathering the modelling techniques that do not fit into the previously defined categories.

An overview of the available studies in the literature is presented in Table 1, where the modelling techniques are classified based on several parameters, described in the following paragraphs. It is important to note that publications of type (IV) are not included in Table 1, and are analysed separately in Section 2.2.1.

Publication year highlights the research efforts over the last decade in exploring alternative modelling approaches to the mooring problem. Within the complete review section, 40 references on the topic are highlighted and discussed, and the trend of these references (categorised in Table 1) clearly illustrates the significant effort in the past ten years to shift towards modelling techniques that differ from classical approaches.

Type leverages the classification proposed in Fig. 2 to provide an overview of the modelling techniques for such systems. Approximately 70% of the analysed studies adopted a Type (I) structure, 22% a Type (II), and 8% a Type (III). It is noteworthy that Type (I) methodologies, serving as passive feedback controls for the system, are not affected by a "filtering" effect, which is inevitable in Type (II) techniques. In particular, in these, the device essentially acts as a band-pass filter, and some mooring components may be neglected. This characteristic could represent a limitation, especially if the model aims to represent ultimate limit state conditions (DNV, 2015), where a faithful representation of snap-load events is crucial. Such nonlinear events can occur significantly faster than the device motion, and thus, may be filtered out. Additionally, if a black-box approach is employed, models tend to be less flexible in Type (II) and (III) scenarios, where minor variations in any device property can compromise the overall response and model validity. Different modelling input/output structures are clearly adopted in related studies; for example, Wang et al. (2023) identifies a mooring force to motion structure (*i.e.*, $\tilde{f}_m/\tilde{x}$), demonstrating an overall good fit between the predicted and target data.

[2] Although in most applications the disturbance field can be referred to as wave exciting conditions, in a general framework, the motion of mooring lines can also be induced by current forces, among others.

[3] The disturbance is due, among others, to the variation of water velocity around the mooring lines which affects, for example, the system drag.

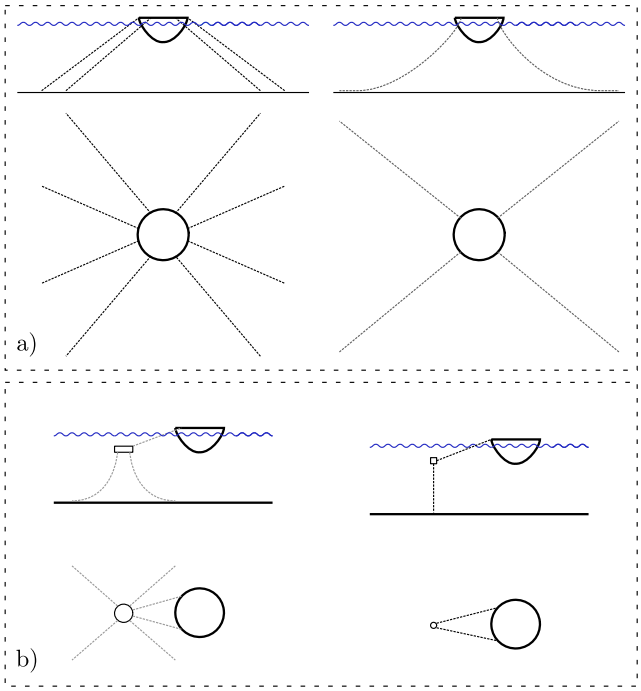


Fig. 3. Schematic representation of the mooring types: (a) Representation of the spread mooring systems, on the left-hand side a taut mooring configuration, on the right-hand side a catenary mooring configuration; (b) Single point mooring, on the left-hand side a catenary anchor leg mooring (CALM), on the right-hand side a taut leg mooring.

Black-box/grey-box models (bb/gb models) reflects the model flexibility, or its reliability beyond the testing configuration. Early studies (Narayanan et al., 1998; Raman and Yim, 2003; Raman et al., 2005) propose a grey-box identification, fitting data from an experimental campaign at Oregon State University. Here, a simplified case study of a floating sphere moored in a spread configuration with springs is analysed. While springs can easily be used to approximate mooring stiffness at reduced scale, the inclusion of such mechanical systems significantly reduces the nonlinear behaviour of the lines. Notably, with the exception of Corrêa et al. (2023b,a), recent works do not propose grey-box models. In Corrêa et al. (2023b,a), the position of an inspecting remote operating vehicle (ROV) is used to tune the parameters of a finite element software to accurately reflect the mooring as-laid layout.

Mooring type refers to the mooring configurations that can be adopted. To keep this study reasonably self-contained, a schematic description is provided in Fig. 3. A detailed comparison of the engineering advantages and limitations of the different mooring configurations falls outside the modelling scope of the present manuscript; the interested reader is referred to the recent review by Jiang (Jiang, 2025) for a comprehensive overview.

To complement the above and clarify the variety of layouts that fall under the spread mooring family, we first distinguish between three broad categories according to the mechanism through which the restoring force is generated. In *taut* configurations, the restoring force is dominated by the axial stiffness of the line, which typically consists of synthetic ropes and works in a nearly straight, pretensioned condition. In *catenary* configurations, the restoring force is instead governed by the line weight and its interaction with the seabed. *Semi-taut* (or hybrid) configurations combine features of both, e.g. by pairing catenary end-sections with a taut synthetic mid-section, and are commonly adopted to trade off restoring nonlinearity, footprint, and pretension. Focusing on the catenary case, the five canonical layouts of a single mooring line are illustrated in Fig. 4. (a) The *free hanging catenary* is

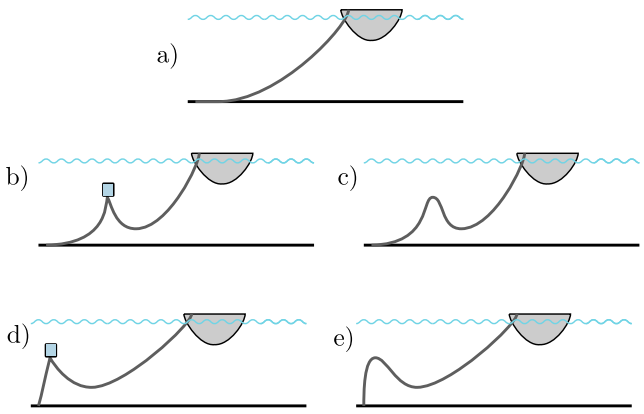


Fig. 4. Canonical layouts of a single spread catenary mooring line: (a) free hanging, (b) lazy-S, (c) lazy wave, (d) steep-S, (e) steep wave.

a simple catenary line with no extra attachments. (b) The *lazy-S* configuration takes advantage of a jumper that reduces the vertical force of the catenary line, thereby decreasing the total restoring force on the device. (c) The *lazy wave* is the flexible version of the lazy-S, where the jumper is replaced by a buoyant section distributed along a flexible riser; the hanging line is more exposed to currents and drag, which can be relevant for the routing of the electrical cable. (d) The *steep-S* is similar to the lazy-S, but with the buoyancy element placed closer to the anchor and a corresponding vertical load on the anchor itself, an option that can be exploited under restrained geometrical boundaries to reduce the anchor radius. (e) The *steep wave* configuration distributes the buoyancy along the catenary section, in analogy with the lazy wave. The choice of the specific layout, together with that of the line material (chains, wire ropes, or synthetic ropes), is driven by the operational depth, the target restoring force, and the redundancy requirements of the specific application. It can be observed that, for spread taut or semi-taut (*i.e.*, hybrid) mooring layouts, though the restoring force can be induced by the axial stiffness nonlinearities (Tsukrov et al., 2005), the overall behaviour of the line can be more linear than in catenary sections, where the restoring force is significantly affected by line-seabed interactions (Niosi et al., 2023; Paduano et al., 2024; Sirigu et al., 2022). It is important to note that nonlinear behaviour in the device response can be significantly higher in spread catenary and single point mooring (SPM) layouts, where the overall response is markedly influenced by, among other factors, low-frequency wave-induced forces (Faltinsen, 1993). Among the studies reviewed, Tang et al. (2015) analyses moored system modes using empirical mode decomposition (EMD) and time-varying modelling techniques based on a short-time Fourier transform (STFT), highlighting the potential of such techniques in identifying system modes.

Target data expresses information about the reference model. Although mooring systems can be simulated, also according to standards (DNV, 2015), using a quasi-static approach, all referenced numerical models employ a finite-element technique. In contrast to the quasi-static approach, the finite-element dynamic method ensures that inertia-related forces are considered, which are crucial especially in defining the response of a catenary mooring system, where the restoring force is driven by the catenary weight (Davidson and Ringwood, 2017). Special mention is made regarding (Giorgi et al., 2016; Davidson et al., 2016), where the target model uses a computational fluid dynamics approach (CFD), *i.e.*, a numerical wave tank (NWT). Although the practicality of such approach is significantly compromised by the required computational cost, the authors evaluate the response of a moored system excited by a chirp-sine signal, including an accurate account on any nonlinearities related to system hydrodynamics, such as *e.g.* viscous forces.

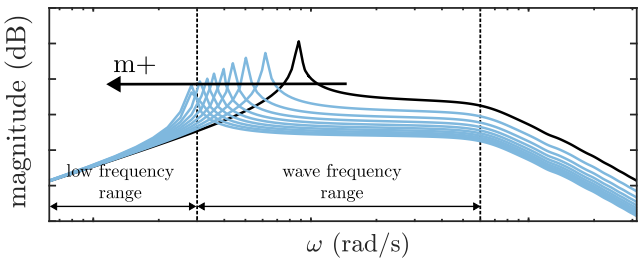


Fig. 5. Influence of the floater mass on the associated response.

Application refers to the floater under investigation in the analysis. The nature of the floater significantly influences the bandwidth of the exciting frequency of the mooring system.

In contrast to larger floating structures, such as FPSO units and FOWT, wave energy systems can be significantly excited by the first-order wave forces within the wave frequency range. This is illustrated in Fig. 5, which clearly shows how the system size, *i.e.*, its mass, affects the response.

Approach outlines the structure of the black-box identification method used. Proper SI modelling requires choosing an appropriate model structure. Although a model based on neural networks (NN) can effectively represent both a linear and a nonlinear phenomenon, it comes with significant computational and mathematical burdens compared to a linear autoregressive approach. Moreover, given the inherently nonlinear nature of moorings, the choice of model structure generally falls into a nonlinear category. It is noteworthy that the most common modelling choice is represented by neural networks, which can take various forms (*e.g.*, recursive NN, deep NN). For a comparison of NN approaches with other model structures, the reader is referred to Zhang et al. (2024), Giorgi et al. (2016), Davidson et al. (2016), Wang et al. (2023) and to the state-of-the-art in SI techniques (Simpkins, 2012; Schoukens and Ljung, 2019; Ljung and Glover, 1981; Sjöberg et al., 1995; Ljung, 2010). We finish by highlighting that in B Paduano et al. (2023) a frequency domain approach is adopted to predict the system response, and the associated, relevant mooring influence has been included by leveraging the associated frequency response.

2.2.1. Mooring modelling - type (IV)

While the overall mooring problem can generally be addressed using an I/O structure, as described in Fig. 2, in some cases, alternative strategies are necessary. Significant research effort is devoted to modelling techniques, aimed at optimising the mooring design problem. For instance, Lee et al. (2021) discusses how an evolutionary algorithm is employed to train a neural network capable of evaluating mooring tension across various configurations. However, a notable gap remains between the available literature and the actual needs of both research and industry. Current research is often constrained to defining optimisation problems with limited parameters, ultimately necessitating a human-in-the-loop approach to design the mooring systems. For a comprehensive overview of available optimisation techniques, the interested reader is referred to Ja'e et al. (2022b).

Typically, the design of a mooring system involves developing a reduced-scale model before creating a full-scale system. By leveraging wave tank experiments, designers can verify and fine-tune any derived mathematical model. However, in ultra-deep conditions (greater than 1000 m), mooring designers face difficulties in conducting wave tank prototyping at representative scales. In such cases, a hybrid modelling technique known as the truncation method can be employed. Described in Kendon et al. (2008), this method uses a hardware-in-the-loop framework to experimentally evaluate the upper part of the mooring, while analysing the lower part of the system numerically. Several challenges can be associated with this approach, particularly at the interface, where designers must adjust the numerical parameters in a grey-box manner while minimising lag (Zhang et al., 2013). For further details on this problem and potential solutions, readers are directed to Wei et al. (2021), Sauder et al. (2018), Wei et al. (2021).

Finally, beyond modelling and simulation-oriented studies, increasing attention has been devoted in recent years to the analysis of moored systems within a structural health monitoring framework. This research direction focuses on exploiting measured responses to infer changes in the system state, rather than on reproducing the full physical behaviour through high-fidelity simulations. Although most simulation schemes have already been presented and discussed, it is worth highlighting the significant research effort of the past few years devoted to SHM applications for mooring systems. In this context, neural networks still account for the vast majority of the proposed approaches. For instance, Fathnejat and Nava (2026), Mao et al. (2025) analyse mooring line tensions with the aim of identifying damaged system states. In a related but distinct application, Yuan et al. (2024) adopts a transformer-based neural network to forecast mooring tensions in the form $f_k \mapsto f_{k+1}$, highlighting the considerable potential of such architectures due to their ability to exploit long time histories and to leverage parallel computation.

2.2.2. Modelling techniques - pro and cons

It is indeed true that a unique model able to provide a faithful representation of the system, with limited identification effort and computational cost, does not exist, especially considering the wide range of application of mooring models. Furthermore, based on the analysis of the literature discussed in the previous section, several conclusions can be drawn.

We begin by noting that, although a comprehensive overview of potential mooring modelling aims is beyond the scope of this study, the broad set of challenges that a mooring designer must face requires significant *adaptability* of the model. One of the major drawbacks of adopting a time-domain identification black-box approach (such as NNs) relates to extrapolation issues. Conventionally, the identification of a model involves dividing the data into a training set ($\approx$ 80%) and a validation set ($\approx$ 20%). Although in many applications a given signal $\hat{u}(t)$ can be divided into training and validation datasets, such as $\hat{u}(t) = [\tilde{u}(t), u^{\star}(t)]$, the significant variation across all available exciting conditions (*e.g.*, wave input conditions from a wave scatter) must be tested in *extrapolation*, *i.e.*, by considering several representative exciting conditions. This issue is addressed in Wang et al. (2022) and Zhang et al. (2024), where the latter trains the mooring model across various sea states and analyses the fit with different ones, which inevitably leads to a loss of fidelity.

Theoretically, SI aims to discover a suitable system that remains representative under diverse excitatory conditions. In this scenario, the definition of the input signal plays a critical role. A noteworthy study that highlights the dogmas of SI is found in Giorgi et al. (2016), Davidson et al. (2016) where, initially, the authors contend with the problem of identifying signals, emphasising their associated importance. This review thus highlights a still-open point in the current literature: the search for innovative modelling techniques and the significant importance for model designers to have a thorough understanding of mooring and floating systems.

3. Mooring response identification - a frequency domain approach

Within this section, and motivated by the detailed discussion provided in Section 2, a novel approach to mooring identification is proposed. Initially, a general framework is discussed and motivated, followed by a representative application case, to demonstrate the technique applicability and limitations.

For clarity, the applicability and the limitations of the proposed framework are stated upfront. The framework is developed and validated for spread taut and semi-taut mooring layouts, where the response is dominated by the radial axial stiffness of the lines and a

Table 1
Data-based modelling of mooring system: review of the existing studies.

Reference	Year	Type	bb/gb	Mooring type	Target data	Application	Approach
Narayanan et al. (1998)	1998	1	gb	spread with springs	experimental	Buoy	–
Gobat and Grosenbaugh (2001)	2001	1	gb	catenary	experimental	FPSO	–
Simoes et al. (2002)	2002	1	bb	SPM	numerical	FPSO	NN
Raman and Yim (2003)	2003	2	gb	spread with springs	experimental	Buoy	–
Raman et al. (2005)	2005	2	gb	spread with springs	experimental	Buoy	–
Pascoal et al. (2005)	2005	1	gb	catenary	numerical	Buoy	–
Pascoal et al. (2006)	2006	1	gb	catenary	numerical	Buoy	–
Guarize et al. (2007)	2007	1	bb	semitatut	experimental	FPSO	NN
Christiansen et al. (2013)	2013	1	bb	catenary	numerical	FPSO	NN
de Pina et al. (2013)	2013	1	bb	semitatut	numerical	FPSO	NN
de Pina et al. (2014a)	2014	1	bb	semitatut	numerical	FPSO	NN
de Pina et al. (2014b)	2014	3	bb	semitatut	numerical	FPSO	NN
Tang et al. (2015)	2015	2	bb	SPM	numerical	FPSO	EMD
Christiansen et al. (2015)	2015	1	bb	catenary	numerical	FPSO	NN
de Pina et al. (2016)	2016	3	bb	taut,catenary	numerical	FPSO	NN
Davidson et al. (2016), Giorgi et al. (2016)	2016	2	bb	–	NWT	WEC	ARX,NN,+
Sidarta et al. (2017)	2017	1	bb	semitaut	numerical	FPSO	NN
Sidarta et al. (2018)	2018	1	bb	semitaut	numerical	FPSO	NN
Yetkin and Kim (2019)	2019	1	bb	semitaut	numerical	FPSO	NARX
Chung et al. (2020)	2020	1	bb	taut	numerical	TLP	NN
Lee et al. (2021)	2021	1	bb	taut,catenary	numerical	FPSO	NN
Qiao et al. (2021)	2021	1	bb	semitaut	numerical	FPSO	NN
Zhao et al. (2021)	2021	1	bb	catenary	numerical	FPSO	NN
Saad et al. (2021)	2021	2	bb	semitaut	experimental	FPSO	NN
Bjørni et al. (2021)	2021	1	bb	catenary	numerical	FOWT	NN
Niosi et al. (2021)	2021	1	bb	catenary	numerical	WEC	NN
Mao et al. (2022)	2022	1	bb	taut, semitaut	experimental	FPSO	NN
do Prado et al. (2022)	2022	1	bb	taut	numerical	FPSO	NN
Wang et al. (2022)	2022	1	bb	semitaut	numerical	FPSO	NN
Corrêa et al. (2023b,a)	2023	1	gb	catenary	experimental	FPSO	–
Wang et al. (2023)	2023	2	bb	SPM	experimental	WEC	ARX,NN,+
Yang et al. (2023)	2023	1	bb	taut	experimental	Barge and ship	NN
Chen et al. (2023)	2023	2	bb	spread with springs	experimental	WEC	AR
Hu et al. (2023)	2023	1	bb	SPM	numerical	Buoy	NN
B Paduano et al. (2023)	2023	1	bb	taut	numerical	WEC	FRD
Zhang et al. (2024)	2024	3	bb	SPM	experimental	WEC	ARX,NARX,+
Mousavi et al. (2024)	2024	2	bb	taut	numerical	FOWT	NN
Kang et al. (2025)	2025	1[a]	bb	catenary	numerical	FOWT	NN

[a] Additional inputs are used to predict mooring tension.

linear, frequency-domain identification structure is appropriate. Catenary systems, mooring layouts with strong nonlinear axial stiffness, configurations subject to significant seabed interaction or slack-line events, and harsh environmental conditions in which the linear assumption breaks down lie outside the validated scope of the present implementation. The modular architecture of the framework is, however, retained in such cases, with the linear model structure replaced by an explicitly nonlinear identification, as further discussed in Section 6.

We begin by addressing the challenge that we aim to bridge in mooring design. As indicated by discussion in Section 2, no single modelling technique currently fills the gap effectively for any application. Furthermore, based on the analysis presented in Section 2, the proposed model can be linked to the following features and limitations:

- The model structure is a type (I) structure, chosen for its greater flexibility compared to other structures. This includes the ability to decouple the mooring model from the hydrodynamics.
- The identification approach entails determining the frequency response of a single mooring line using a black-box approach. However, the entire mooring system is parametrised based on the orientation of the lines, and the transition from a non-parametric to a parametric form is inherently linked to the line axial stiffness. This connection steers the model towards a semi-physical grey-box model.
- Given the wide variety of spread mooring configurations, and their associated redundancy features, this model is particularly suited for such layouts, excluding SPMs.
- To demonstrate the generality of the formulation, the methodology is first applied to a pitching WEC, whose resonant dynamics induce large-amplitude motions and therefore provide a stringent test case for system identification. The same framework is subsequently extended and validated using experimental data from a reduced-scale FOWT, highlighting its applicability across different floating energy systems.

Please note that, while the main limitation on the proposed methodology relies on the application on spread mooring type, in Section 4 a taut mooring system is presented. The aim of such application study is related to exposing how a straightforward linear identification process can faithful represent a mooring response. From a general perspective, when addressing the identification of catenary or hybrid mooring systems, where geometric nonlinearities play a significant role, the overall identification framework may remain unchanged, while the model structure adopted for the identification process must evolve towards a nonlinear formulation in order to faithfully represent the mooring response.

3.1. General modelling framework

We begin by analysing the general modelling framework proposed. Notably, except for SPMs where the mooring configuration cannot be considered symmetrical relative to the device, moorings are predominantly set up in a spread configuration (see Table 1). This preference is largely due to the necessity for redundancy in mooring lines (DNV, 2015), which is more readily achieved in such configurations. Mooring

arrangements in a symmetrical pattern[4] allows for the simplification of identifying just one mooring line and applying the response across multiple conditions. This assumption significantly simplifies the identification problem, reducing it from the need of identifying several mooring lines to just one. However, if this assumption does not hold due to the complexity of the mooring layout, such as when the mooring lines differ significantly from one another (*e.g.*, due to varying anchor depths or bathymetric conditions), each mooring line should be identified individually. It is important to note that the motion of these lines is uncorrelated, meaning there is no mutual interaction among the lines. Furthermore, each mooring line is connected to the floating structure fairlead via a spherical joint, which ensures that the restoring force direction is aligned axially according to the position of the last mooring segment. The restoring force effect at the top end of the mooring line can be summarised as follows:

$$f_{ml} = f_{EA} + f_{drag} + f_{inertia}, \tag{4}$$

where the force components include the axial stiffness (f_{EA}), the effects of velocity and viscosity (f_{drag}), and the inertia term ($f_{inertia}$). In a general modelling framework, these forces can be evaluated using the Morison formulation for slender bodies (J.R.R. Morison et al., 1950; J.R. Morison et al., 1950), which provides an approximation of the line restoring force as:

$$\begin{aligned} \tilde{f}_{ml} &= \tilde{f}_{EA} + \tilde{f}_{drag} + \tilde{f}_{inertia}, \\ \tilde{f}_{EA} &\propto k(x)x, \\ \tilde{f}_{drag} &\propto \dot{x}|\dot{x}|, \\ \tilde{f}_{inertia} &\propto \ddot{x}. \end{aligned} \tag{5}$$

Although the dynamics of the entire mooring line can be complex, it is noteworthy that, due to the nature of the connection with the floating unit, the force at the fairlead is oriented tangentially to the catenary shape. This orientation is governed by a balance of forces primarily influenced by the catenary weight and the associated line stiffness. The entire problem can be analysed according to different frames of reference (FoRs) as depicted in Fig. 6. This approach allows us to describe the fairlead motion, starting from the device motion (O_b motion with respect to O_{global}), using spherical coordinates in the anchored, fixed, FoR (*i.e.* the O_a centred FoR).

Note that, the angle θ represents precisely the tangential direction of the catenary. This can be defined by the last section (*i.e.*, the last segment using the common modelling technique) of the mooring line, or by leveraging the ratio between the force caused by the weight of the line and the total force.

These changes of coordinates ensures us to have the opportunity of representing the forces on the fairlead in the line axial and tangential direction. All the described process is schematically represented in Fig. 7, where it is possible to appreciate that, when identifying the mooring system g_m, the full problem can be solved, after few changes of coordinates, in terms to the approximation of a single line model:

$$g_{ml} = g_{ml,1} = g_{ml,n_f}, \tag{6}$$

in which $n_f \in \mathbb{N}^+$ represents the number of fairleads. Given the large variety of mooring line configurations, assuming a unique model structure, able to capture the dynamics of any response while keeping the identification process as simple as possible, is far from being trivial.

As the reader will notice, with very few limiting assumptions, the identification problem can be simplified significantly. For instance, given that the lengths of the mooring lines are generally much larger than the floater offset (the motion of O_b relative to O_{global}), it is reasonable to assume that the φ component of the force is significantly smaller compared to other contributions, which are functions of line inertia, drag, and stiffness (see Eq. (5)). Additionally, the line inertia force, driven by the weight (and added mass) of the hanging line length, can be assumed to be constant in the case of semi-taut or taut lines. This discussion leads us to define the fairlead force as $\tilde{f}_{ml} = \tilde{g}_{ml}(\rho, \theta_0)$, in which θ_0 can be determined as a function of the line total force to the fairlead and the line hanging weight. However, as will be detailed in the next section through a representative case study, the characteristics of the proposed modelling framework can be analysed as long as the model $\tilde{g}_{ml}$ remains linear. Furthermore, the response of g_{ml} can be computed as a function of a single parameter. This implies that, by neglecting the integration of θ, which can be assumed constant in the case of taut or semi-taut moorings, the identification problem transitions from a multi-input-multi-output (MIMO) representation to a single-input-single-output (SISO) format.

We acknowledge that the physical derivation presented above may appear more involved than the resulting mathematical formulation. The framework admits an equivalent and more compact interpretation as the projection of the line response onto its principal orthogonal modes, which is, in general, a MIMO description. For taut and semi-taut mooring layouts, the first such mode is aligned with the radial coordinate ρ and dominates the response, while the remaining modes are negligible: the resulting identification problem therefore reduces to a SISO model in ρ.

In a general modelling framework, defining a single model structure is impractical, yet several key considerations can be highlighted based on the assumptions made in Section 2.2.2 and presented in the following:

- **Input exciting conditions**: The definition of the input signal $\tilde{u}$ can be determined by leveraging the I/O map that links wave elevation to device motion (*i.e.,* g_d in Fig. 3).
- **Model structure**: The model structure g_{ml} is considerably simpler for taut or semi-taut configurations, where the linear assumption generally holds, as noted in Section 4. A representative model in such scenarios can be expressed as $g_{ml}(\rho)$. However, catenary mooring systems, where variations in line length laid on the seabed and more complex layouts are encountered,[5] still require a dedicated analysis to define an appropriate, nonlinear, model structure.
- **Validation criteria**: Similar to the input $\tilde{u}$, the definition of the validation signal $u^\star$ can be achieved by leveraging the I/O map that links wave elevation to device motion, analysing a representative set of exciting conditions for both operative and extreme sea states.

This structured approach to model development, leveraging the physical links with the governing Eq. (5), ensures the achievement of a more representative model.

4. Numerical identification: the PeWEC

As a case study, a pitching wave energy converter (WEC) is adopted and analysed in detail. WECs are a useful test bed for the proposed identification framework because they typically undergo large-amplitude motions over a broad frequency range: the wave-frequency band, where the device resonance (on which power absorption relies) enhances the response, and the low-frequency/second-order range, which is the band most relevant to mooring design through mean offsets and slow-drift motions in surge and sway. The combination of these two contributions excites the mooring system across the entire bandwidth of interest and

[4] Although in a final design mooring lines may differ from each other, being influenced by factors such as a non-flat seabed, in a preliminary general design, a symmetrical pattern implies that the response of any mooring line is the same.

[5] It should be noted that even in more complex mooring layouts, the line model can be described as $g_{ml}(\rho, \theta)$, with the force variation in φ being necessarily small.

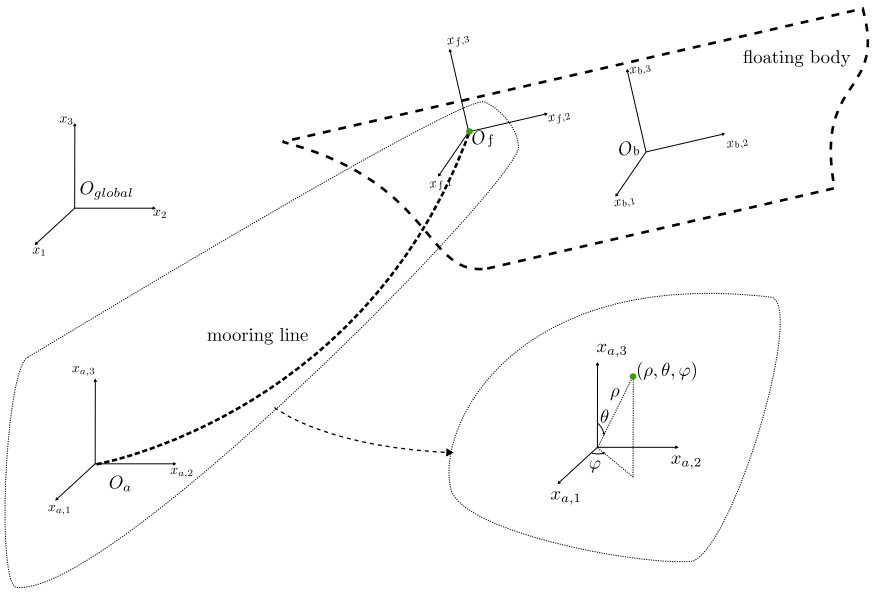


Fig. 6. Representation of the FoRs: the FoR centred in O_{global} represents the inertial global FoR, those centred in O_f and O_b are the local FoRs describing the body and the associated fairlead motion, respectively, and, finally, the FoR centred in O_a describes the anchor FoR.

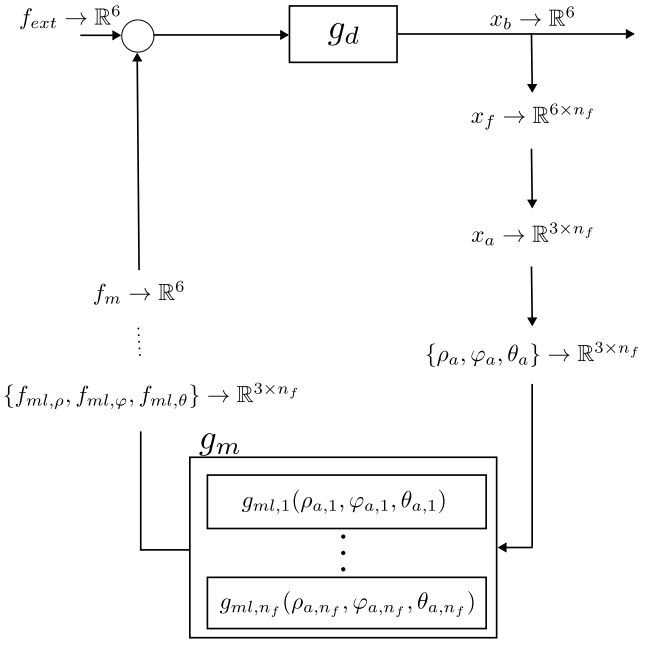


Fig. 7. Schematic representation of the simulation scheme outlining the required changes of coordinates.

therefore provides a stringent scenario for the proposed framework. A detailed description of the device, including experimental and numerical analysis of both the mooring system and the device response, is provided in Paduano et al. (2024). The properties of the floater are summarised in Table 2. For a more comprehensive description of the system, the reader is referred to Bruno Paduano et al. (2023).

The device is moored using a 4-lines, spread, taut station-keeping system, which consists of a line comprising three different sections: chain, polyester, and chain. These sections have lengths of $l_1 = 5$ m, $l_2 = 138$ m, and $l_3 = 10$ m, respectively. The mooring configuration is depicted in Fig. 8, and the associated properties are detailed in Table 2. The anchors are distributed according to the anchor radius (see Table 2), describing an angle of 30° with the x_1 axis (see Fig. 8).

Table 2
Floater, mooring, and site properties.

Parameter	Unit	Value
hull length	m	14.8
hull width	m	22.5
hull height	m	7.4
CoG x_3 position	m	−1
draft	m	4.81
pitch inertia moment	kgm^2	29.9e6
roll inertia moment	kgm^2	55.3e6
yaw inertia moment	kgm^2	72.1e6
device mass	kg	1.12e6
chain diameter	m	0.06
chain axial stiffness	kN	363.6e3
polyester diameter	m	0.12
polyester axial stiffness	kN	15.7e3
jumper net buoyancy	kg	2000
anchor radius	m	151
mooring pretension	kN	158
number of mooring line	–	4
water depth	m	32

Please note that, while the polyester section provides the required stiffness for the taut mooring configuration, the catenary sections help avoid collisions of the synthetic line with the seabed or working in the splash zone (DNV, 2015). We would like to note that this mooring system has been designed for the Pantelleria site, in southern Italy, in accordance with the environmental conditions proposed in Section 4.3.

4.1. Numerical model

The target reference model is developed using OrcaFlex, a commercial solver capable of solving the coupled dynamics of moored objects. The hydrodynamic problem is addressed using a boundary element method (BEM) approach, *i.e.*, by solving the equation known as Cummins' equation (Cummins, 1962):

$$m\ddot{x}_b = f_e + f_r + f_h + f_{md} + f_m, \tag{7}$$

$$f_r(t) = -A_\infty\, \ddot{x}_b(t) - \int_0^t K(t-\tau)\, \dot{x}_b(\tau)\, d\tau, \tag{8}$$

in which $x_b : \mathbb{R}^+ \to \mathbb{R}^6, t \mapsto x_b(t)$ represents, according to the nomenclature used in Section 3, the position of the floating body,

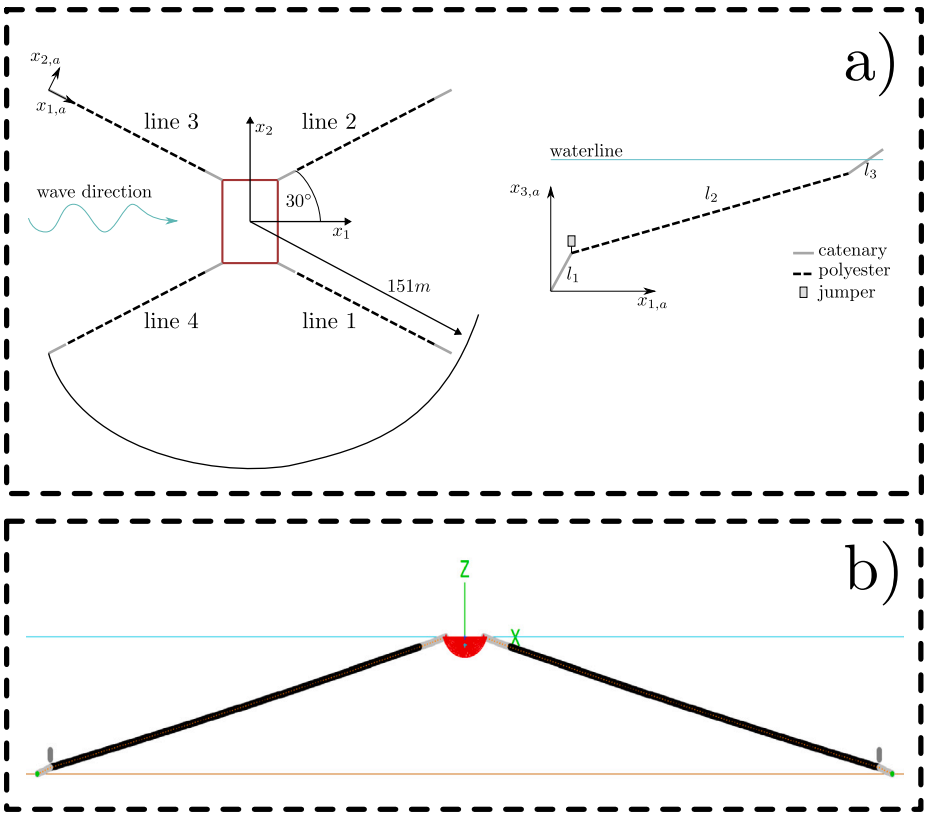


Fig. 8. (a) Moored device scheme: details on the single line sectioning are highlighted on the right-hand-side. Note that the line indices used in the validation stage are indicated. (b) Mooring side-view in OrcaFlex, with the device in equilibrium position.

$m \in \mathbb{R}^{6\times6}$ is the device inertial matrix, and $\{f_e, f_r, f_h, f_m\} : \mathbb{R}^+ \to \mathbb{R}^6, t \mapsto \{f_e(t), f_r(t), f_h(t), f_m(t)\}$ are the excitation, radiation, hydrostatic force, and mooring force, respectively. In Eq. (8), $A_\infty \in \mathbb{R}^{6\times6}$ is the added mass matrix at infinite frequency, and $K : \mathbb{R}^+ \to \mathbb{R}^{6\times6}$ is the radiation impulse response (memory kernel) evaluated through the Ogilvie functions (Ogilvie, 1964); the convolution term in Eq. (8) provides the velocity-dependent damping contribution of the floating body to Eq. (7). The term $f_{md} : \mathbb{R}^+ \to \mathbb{R}^6, t \mapsto f_{md}(t)$ represents the drift forces acting on the device, which are nonlinear terms related to the squared value of the wave height (Faltinsen, 1993).

The hydrodynamic model of the floating body is computed by the BEM solver OrcaWave (v. 11.4c) using a potential-flow formulation. The body mesh is generated with two-plane symmetry (xz and yz), so that one quarter of the hull is discretised with approximately 4000 panels, meeting the validation criterion of at least five panels per wavelength for the wave conditions representative of the analysed scenario. The hydrodynamic transfer functions are evaluated on 999 frequencies in the range 0.01 to 5 rad/s (step 0.005 rad/s). The panel-pressure outputs are converted into the time-domain hydrodynamic contributions of Eqs. (7) and (8) via the Ogilvie functions. Further details on the floater hydrodynamics are reported in Paduano et al. (2024).

The mooring system is implemented in OrcaFlex using the lumped-mass line model, with each line section discretised with a fine segmentation of 1 m. The seabed is modelled as a flat surface; its contribution is, however, negligible for the considered taut mooring configuration, in which the synthetic line operates entirely above the seabed. The hydrodynamic coefficients of the line elements (drag and added mass) are taken from the OrcaFlex defaults for the chain and synthetic-rope sections. Numerical integration is performed with an implicit time step of 0.1 s; the segmentation and the time step have both been verified against halved-resolution runs, with negligible differences observed in the fairlead force time histories. The mooring pretension reported in Table 2 is enforced by adjusting the unstretched line length at the beginning of each simulation.

A schematic representation of Eq. (7) is reported in Fig. 9, where the linear BEM model provides, by leveraging the Ogilvie's functions (Ogilvie, 1964), both linear g_e and g_d, and the nonlinear g_{md} map, in a non-parametric form.

To keep this manuscript reasonably self-contained, the main properties of the dynamical system are included herein. In Fig. 9, the system frequency responses in surge, heave, and pitch are included. We would like to remark that these degrees of freedom represent the most relevant ones for a pitching wave energy converter, as pitch, being also hydrodynamically coupled with surge, is the primary motion responsible for energy production. Please note that, from a general perspective, the frequency response is defined as the BEM-based one, *i.e.*:

$$g_{ow} = g_e g_d, \tag{9}$$

where $g_{ow} : \mathbb{R}^+ \to \mathbb{C}^6, \omega \mapsto g_{ow}(\omega)$ represents the so-called response amplitude operator evaluated by means of OrcaWave, a BEM solver. Finally, the mooring system characteristic tension-offset diagram is presented in Fig. 10, where in a quasi-static manner the tensions are diagrammed by means of pull-out tests, recording the resulting net force at the device CoM. Please note that around the equilibrium position, the link between device offset and the resulting tension is significantly nonlinear, while far away from the equilibrium position, a linearity assumption holds, considering that the force exerted by the bow-lines is predominant.

Please note that, while the pull-out test is based on several hypotheses and only analyses a direct motion-to-force link without describing coupling or dynamic terms, it still remains a nonlinear process. This highlights the importance of properly describing the I/O model.

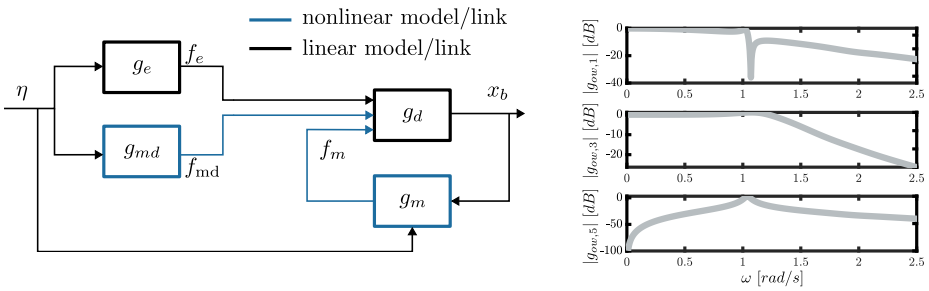


Fig. 9. On the left-hand-side: schematic representation of the simulation target model. The nonlinearities are remarked in blue. On the right-hand-side: the device response amplitude operators in surge, heave, and pitch motion.

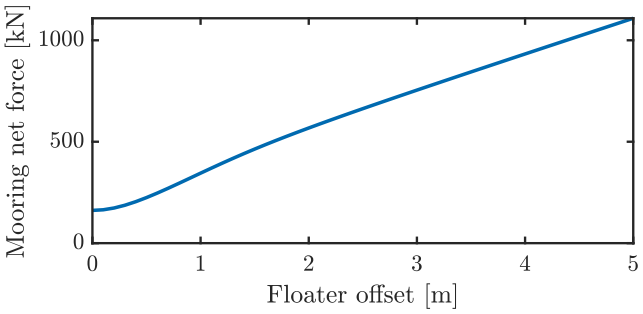


Fig. 10. Mooring system pull-out test.

4.2. Data-based identification of a single line model

In this section, the identification process is discussed. The starting point of the identification procedure relies on the reference target model, which is constituted by the OrcaFlex-based model described in Section 4.1. Consequently, a representative set of input conditions can be defined to generate a set of I/O data by executing the target model. This data characterises the fairlead motion-to-force map of a single mooring line. From this set of data, the frequency response map can be generated, and subsequently, the associated parametric form can be identified.

Since only the single line transfer function is defined so far, the entire identified mooring model can be constructed by spreading the single line model considering the respective angles, as described in Section 3.1. The entire moored OrcaFlex model is then run outside the identification set across a broader set of characteristic exciting inputs for validation purposes. Accordingly, the identified full model is run in an uncoupled manner, imposing the OrcaFlex device motions and comparing the results to the latter in terms of fairlead tensions and net mooring forces. The identification procedure is also depicted in Fig. 11.

According to the modelling framework and the described SI techniques (in Sections 2.1 and 3.1, respectively), the remainder of this chapter is organised into three sections: input exciting conditions, model structure, and validation criteria.

Input exciting condition

Aiming to generate a representative $\tilde{u}$ provides informative data for identification, the following approach is employed: A quantification of the device motion is achieved by using the linear model from the BEM solver, with the wave spectra imposed as input, *i.e.*:

$$S_{x_b} = G_r S_\eta G_r^*, \tag{10}$$

in which, $S_{x_b} : \mathbb{R}^+ \to \mathbb{R}^6, \omega \mapsto S_{x_b}(\omega)$ represents the response spectrum and $S_\eta : \mathbb{R}^+ \to \mathbb{R}, \omega \mapsto S_\eta(\omega)$ the wave spectrum. The map $G_r : \mathbb{R}^+ \to \mathbb{C}^6, G_r \mapsto G_r(\omega)$ is the linear map that links the wave elevation to the device motion (also known as response amplitude operator), and it can be achieved by means of BEM solvers. Accordingly, starting with a significant set of characteristic exciting conditions, the device response and consequently the associated fairleads response in spherical coordinates (as described in Section 3.1) can be determined in terms of amplitude and frequency bandwidth. This information is used to define a representative excitation signal as a Schroeder phase multisine signal (Schoukens et al., 1988). This type of signal is chosen for its periodicity and bounded spectrum, which are advantageous features for the modelling purposes described, see Paduano et al. (2022).

Model structure

In an effort to simplify the model structure, the system is identified using the empirical transfer function estimate (ETFE), which leverages the Fourier transform of the I/O data. Therefore, in this section, we describe the lower left-hand side of Fig. 11, which shows the ETFE obtained by exciting the single mooring line under tailored excitation conditions. The ETFE, denoted as $\tilde{G}_{ml} : \mathbb{R} \to \mathbb{C}^{3\times3}, \omega \mapsto \tilde{G}_{ml}(\omega)$, represents the I/O relationship between the forces described in spherical coordinates and the fairlead motion, described by $\{\rho, \theta, \varphi\}$. Following this I/O relationship, the frequency response matrix can be described as outlined in Section 2.1:

$$Y(\omega) = \tilde{G}_{ml}(\omega)\tilde{U}(\omega), \tag{11}$$

which can be rewritten as:

$$\begin{bmatrix} F_\rho \\ F_\theta \\ F_\varphi \end{bmatrix} = \begin{bmatrix} \tilde{G}_{\rho\rho} & \tilde{G}_{\rho\theta} & \tilde{G}_{\rho\varphi} \\ \tilde{G}_{\theta\rho} & \tilde{G}_{\theta\theta} & \tilde{G}_{\theta\varphi} \\ \tilde{G}_{\varphi\rho} & \tilde{G}_{\varphi\theta} & \tilde{G}_{\varphi\varphi} \end{bmatrix} \begin{bmatrix} \hat{\rho} \\ \hat{\theta} \\ \hat{\varphi} \end{bmatrix}, \tag{12}$$

where each entry $\tilde{G}_{ij}(\omega)$ denotes the empirical transfer function from input $\hat{j}$ to output F_i, with $i, j \in \{\rho, \theta, \varphi\}$. The magnitude of the matrix $\tilde{G}_{ml}$ is shown in Fig. 11, where the contributions of the variables $\{\rho, \theta, \varphi\}$ to the resulting line forces $\{F_\rho, F_\theta, F_\varphi\}$ can be appreciated. Considering the physical properties of the mooring system, several observations can be made:

1. $\tilde{G}_{\rho\rho}$ has a constant amplitude, *i.e.*, it can be approximated by a first-order system. This implies a linear constant stiffness contribution to the restoring force.
2. $\tilde{G}_{\rho\theta}$ and $\tilde{G}_{\rho\varphi}$ have marginal contributions to the restoring force, considering the very low variation in the variables φ and θ. This minimal variation is due to $\frac{\text{line length}}{\text{device motions}} \gg 1$.
3. Based on the assumption stated in point 2, it can be inferred that all other contributions can be neglected.

Within this assumptions, the frequency response $\tilde{G}_{ml}$ can be approximated by its $(1,1)$ entry $\tilde{G}_{\rho\rho} : \mathbb{R} \to \mathbb{C}$. Once the parametric response is identified, $\tilde{G}_{\rho\rho}$ is approximated by a transfer function $\tilde{g}_{ml} : \mathbb{R} \to \mathbb{C}, s \mapsto \tilde{g}_{ml}(s)$ in a parametric form, aiming to characterise the response $\tilde{y}(t)$ as that of a dynamic model. It is important to note how an identification process, which can inherently be complex, has been reduced to the identification of a SISO system by leveraging an ETFE description. We would like to emphasise that the identified $\tilde{G}_{ml}$ captures the overall behaviour of the entire mooring line, despite the significantly different properties of each section and/or attachment point.

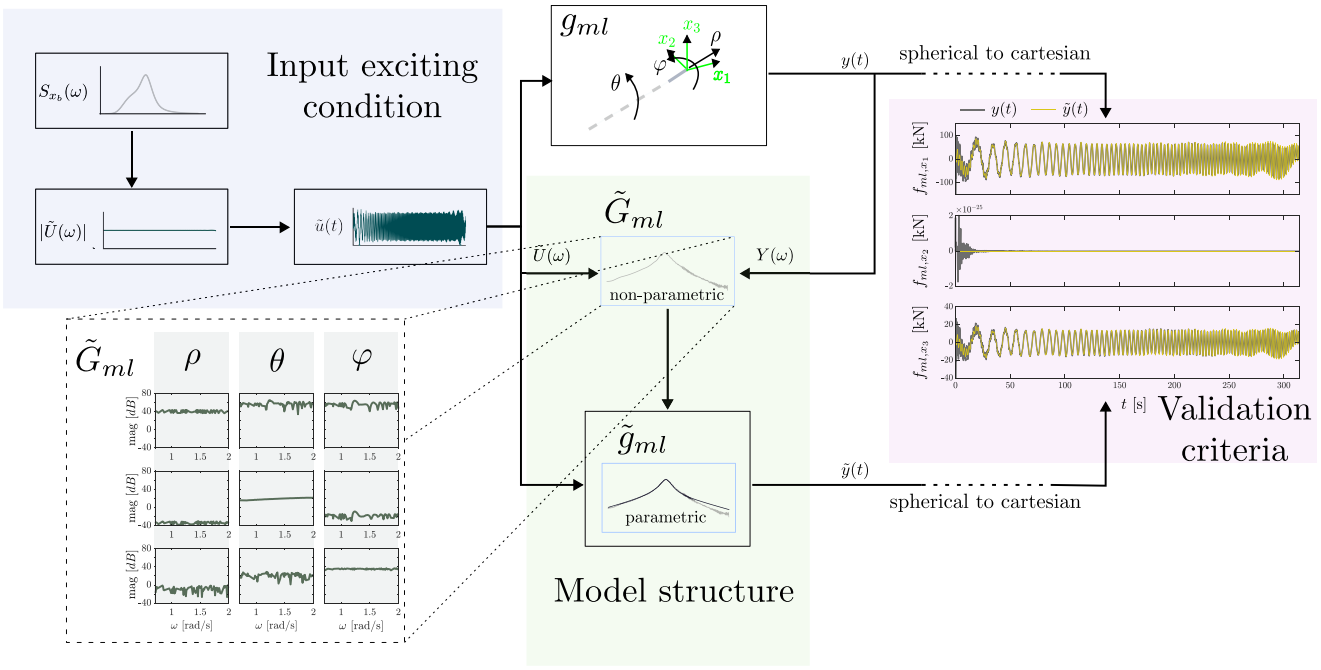


Fig. 11. Definition of the mooring line frequency response: following the framework described in Section 2, the input exciting conditions, model structure, and validation criteria are outlined. In the bottom-left corner, the non-parametric response of the mooring line $\tilde{G}_{ml}$ is shown.

Validation criteria

To validate the assumptions described in the previous section, and evaluate the linearisation process, an initial comparison is presented, involving the forces on the fairlead, which are expressed in Cartesian coordinates. It can be observed in the right had-side of Fig. 11 that, each component effectively represents the line response, achieving a normalised root mean squared accuracy (NRMSA) index of 91% for the force component in x_1 and 84% for x_3, defined as:

$$\text{NRMSA} = 1 - \frac{\|q - q^{\bullet}\|}{\|q - \mu_q\|}, \tag{13}$$

where NRMSA $\in \mathbb{R}$, $\mu_q \in \mathbb{R}$ represents the mean value of the reference signal, and $\{q, q^{\bullet}\} : \mathbb{R}^+ \to \mathbb{R}, t \mapsto \{q(t), q^{\bullet}(t)\}$ are the reference and simulated signals, respectively. Please note that, in Fig. 11, the zero-mean force signals are presented. In the general case discussed in Section 4.3, static pretension is added to F_ρ, and the θ angle is modified according to the static conditions (*e.g.* $\theta \approx \theta_0$ according to Section 3), which entails considering the influence of the line weight (*i.e.*, the orientation of the last line segment, as detailed in Section 3.1).

It is crucial to note that, in the scenario presented here, the representativeness of $\tilde{g}_{ml}$ needs to be carefully examined in extrapolation conditions, where problems may arise. Moreover, while the identification process described so far focuses on achieving a SISO model for a single line, the generalisation of the entire mooring response as depicted in Section 3.1 requires validation with the complete model.

4.3. Results

Within this section, the identified mooring line model has been extended to construct the mooring configuration described in Section 4, with the lines arranged symmetrically. To evaluate the model performance under various environmental conditions, real site data are analysed.

Wave data is sourced from the ERA5 online database (Hersbach et al., 2020) and is presented as energy density scatter in Fig. 12. Here, the energy density of a wave is calculated as $0.49 O_{cc} T_e H_s^2$, where T_e and H_s are the wave energy period and the significant wave height, respectively (World Meteorological Organization, 1988), and $O_{cc} \in [0, 1]$

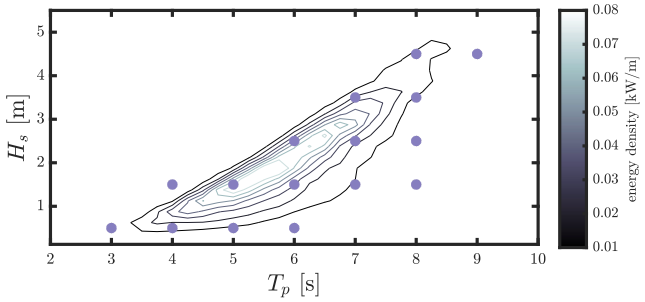


Fig. 12. Pantelleria wave energy scatter. The waves adopted are marked with circles and detailed in Table 3.

represents the wave occurrence. To define a set of representative waves for the Pantelleria site, the most energetic waves are selected from the scatter and listed in Table 3. To generalise the input conditions, a random angle, described relative to the device bow direction (*i.e.*, $Dir \in [0, 90]$), has been assigned to each wave, to excite the system under asymmetrical conditions. Please note that significant influence on the mooring response can be attributed to the mean drift forces, which may cause different equilibrium-in-plane conditions of the floater, thus resulting in significant variation of the mooring response. All simulations are conducted using OrcaFlex, analysing a time-span of 600s[6] for each condition. Subsequently, the OrcaFlex motions are imported and imposed on the full mooring model ($\tilde{g}_m$), and the results are compared. The accuracy index, evaluating the line end force at the fairlead, is reported in Fig. 13. Given the wide range of exciting conditions, the identified model successfully represents the system dynamics, achieving an average fit value of 90%. The fit index and the wave height appear to be correlated, as the lowest fit values occur with higher wave heights. These conditions need to be analysed in more detail since, as given the model structure (*i.e.*, a type (I) structure, see Section 2.1), the

[6] The time span of 600 s is chosen to be statistically representative of the energy-producing motion, as suggested in Merigaud (2018).

Table 3
Definition of the input wave conditions. The wave direction is referred to the device bow.

wave index	T_p [s]	H_s [m]	Dir [°Bow]
1	5	1.5	8
2	6	1.5	74
3	6	2.5	63
4	7	2.5	28
5	7	3.5	86
6	8	3.5	3
7	7	1.5	39
8	4	0.5	34
9	5	0.5	69
10	4	1.5	72
11	8	4.5	17
12	8	2.5	44
13	3	0.5	40
14	8	1.5	58
15	9	4.5	64
16	6	0.5	68

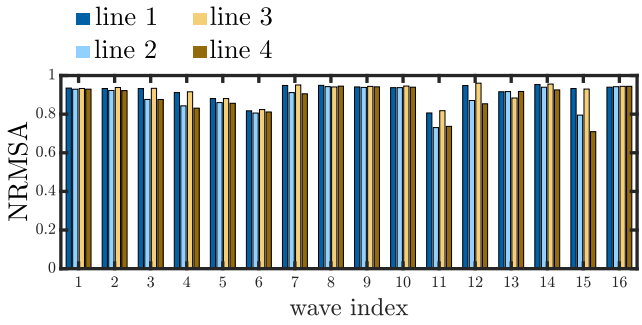


Fig. 13. NRMSA of the mooring line forces at the device fairleads. Wave indices refer to Table 3, and for each wave index, the bars represent the four device fairleads.

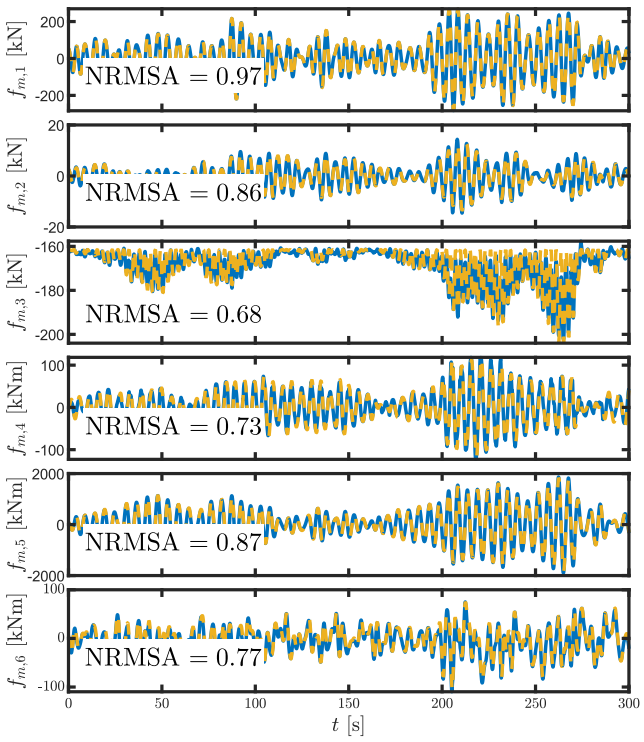


Fig. 14. Mooring net forces at the device CoM, time histories for wave 1. Indices 1 to 6 correspond to surge, sway, heave, roll, pitch, yaw. Yellow dashed: $\tilde{y}(t)$; blue: $y(t)$.

hydrodynamic nonlinearities of the floater do not influence the model faithfulness, suggesting that these inconsistencies may be attributed to two factors:

1. The wave field has a significant impact on the line dynamics at larger wave heights.
2. The linear assumptions of the model are challenged by significant device motions, which inherently move towards slack conditions, pushing the required modelling techniques beyond linear theory.

Although the first factor appears to be correct in theory, given that simulations are conducted without any current phenomena, the associated drag effect of the lines should be marginally affected only by the wave kinematics field.

The data-based model described should be evaluated considering all six components of the force vector f_m at the device CoM. In Fig. 14, as an explanatory example, the time histories for these components are reported for wave 1, *i.e.* the most energetic wave at the Pantelleria site. While the identified mooring model faithfully predicts most of the mooring dynamics, slight discrepancies arise considering $f_{m,3}$, where limitations can be attributed to the SISO structure of the model given that the influence of θ significantly affects such a force component.

To keep this study reasonably self-contained, we conclude by analysing the system and mooring response (associated with the target model) as reported in Fig. 15. A detailed representation of sea state 11, which corresponds to the sea state with the highest mean device planar offset (see Fig. 15), is provided. For this sea state, the mooring force evaluated at the fairlead is reported, along with the device offset (evaluated as the planar distance from the equilibrium position) in both the time and frequency domains. In the frequency domain, a distinction is made between the wave frequency region, where the device response is primarily generated by linear wave forces, and the low-frequency region, where wave sub-harmonics generate second-order loads. This low-frequency region is a key aspect in the design of a mooring system, as resonance conditions for surge and sway motions occur here.

5. Experimental identification: a semisub FOWT

This section demonstrates the applicability of the proposed approach through experimental testing, extending the application scenario to a different floating structure, *i.e.* a floating offshore wind system. A comprehensive description of the experimental campaign and test facilities is provided in Niosi et al. (2025); here, only a concise overview of the setup is reported to keep the manuscript reasonably self-contained.

The experimental campaign was conducted on a 1:96 reduced-scale FOWT model, designed to investigate the dynamic response of a semi-submersible platform equipped with a taut-leg mooring system under realistic environmental loading conditions. The model is based on the DeepCWind semi-submersible concept and was tested at a geometric scale of 1:96, selected to comply with the dimensional constraints of the experimental facility. The main inertial, hydrostatic, and mooring properties of the reduced-scale model are summarised in Table 4.

The floating structure consists of four columns connected by a rigid frame: a central column supporting the wind turbine tower and three outer columns equipped with heave plates, which also act as fairlead attachment points for the mooring lines. The assembled model and the corresponding mooring experimental mock-up are shown in Fig. 16.

The mooring system comprises three equally spaced taut lines, representative of the optimised full-scale configuration and reproduced at model scale by matching the axial stiffness governing the global station-keeping behaviour. Two alternative layouts were investigated. The first employs linear springs to reproduce a constant-stiffness response, while the second uses nylon lines to capture the non-linear stiffness behaviour

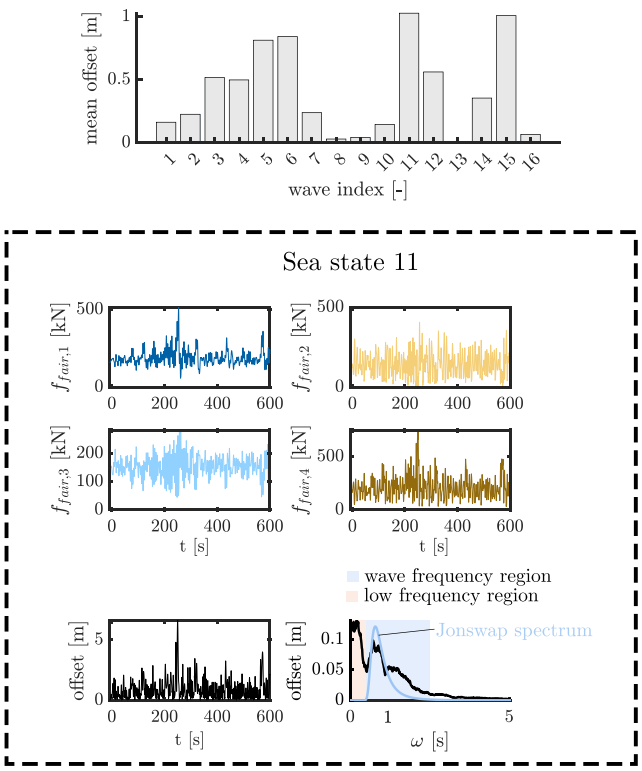


Fig. 15. Top: mean planar offset of the device for all weather conditions. Bottom: sea state 11, mooring force at the fairlead for each line, and device offset in time and frequency domain (with the JONSWAP exciting spectrum to delimit the wave and low-frequency regions).

typical of synthetic ropes. In the spring-based configuration, the elastic element is characterised by an unstretched length of 52 mm and a linear stiffness of 30.5 N/m (Table 4), enabling a controlled and repeatable representation of the target axial rigidity.

The experimental programme included regular, irregular, multisine, free-decay, and limit-state tests, allowing both system identification and performance assessment under operational, extreme, and accidental loading scenarios. The resulting dataset provides a comprehensive benchmark for the validation of numerical models and for the analysis of taut-leg mooring systems applied to floating offshore wind turbines. To maximise reproducibility and scientific impact, all experimental data have been made openly available through the repository described in Niosi et al. (2025).

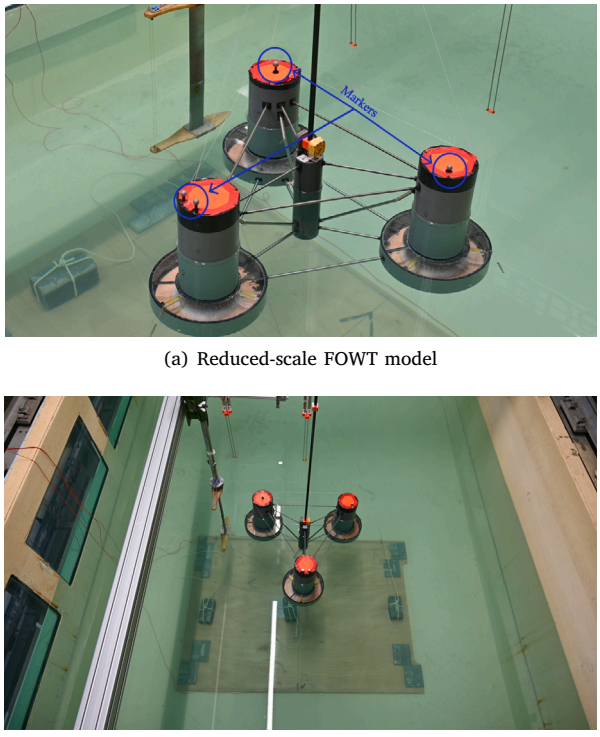
Building on the modelling assumptions and identification framework introduced in Section 4, the same model structure is adopted here. The identification and validation conditions specific to the experimental campaign are described in the following subsections.

5.1. Identification of the experimental line

While the numerical framework offers a high degree of flexibility in the identification procedure, such as the possibility to isolate and analyse individual force components, this level of decomposition is not achievable in an experimental setting. Consequently, a number of simplifying assumptions are required, which have already been assessed and validated in Section 4. Accordingly, based on Eq. (12), and given the taut nature of the mooring system, the force-to-motion frequency response is assumed to be dominated by the radial component. Under this assumption, the identification of the mooring line can be formulated as a SISO problem, with the radial force acting as the input and the corresponding floater motion as the output.

Table 4
Reduced-scale properties of the floating model and mooring system.

Parameter	Unit	Value
Floating body properties		
total mass	kg	15.90
centre of gravity from keel	mm	128
free-floating draft	mm	208
roll inertia moment I_{xx}	kg m^2	1.77
pitch inertia moment I_{yy}	kg m^2	1.79
yaw inertia moment I_{zz}	kg m^2	1.22
Mooring system properties		
number of mooring lines	–	3
pre-tension per line	N	1.7
maximum design load	N	3.62
axial stiffness EA	N	19.92
axial stiffness	N/mm	0.032
outer diameter	mm	4.03
nylon rope length	m	0.63
water depth	m	1.04
Spring element		
spring unstretched length	mm	52
spring stiffness	N/m	30.5
Fairlead and anchor geometry		
fairlead depth	m	0.146
anchor depth	m	1.042
fairlead radius	m	0.43
anchor radius	m	0.78



(a) Reduced-scale FOWT model

(b) Mooring Experimental mockup

Fig. 16. Mooring configurations sketch.

Furthermore, the definition of the excitation conditions cannot replicate those adopted in Section 4, as it is not possible to directly prescribe the fairlead motion in the experimental setup. Although multisine wave conditions were tested during the experimental campaign to characterise the floating system following a *Type II* identification scheme (see Fig. 2), the resulting fairlead motion is inherently filtered by the floater dynamics. As a consequence, the effective excitation

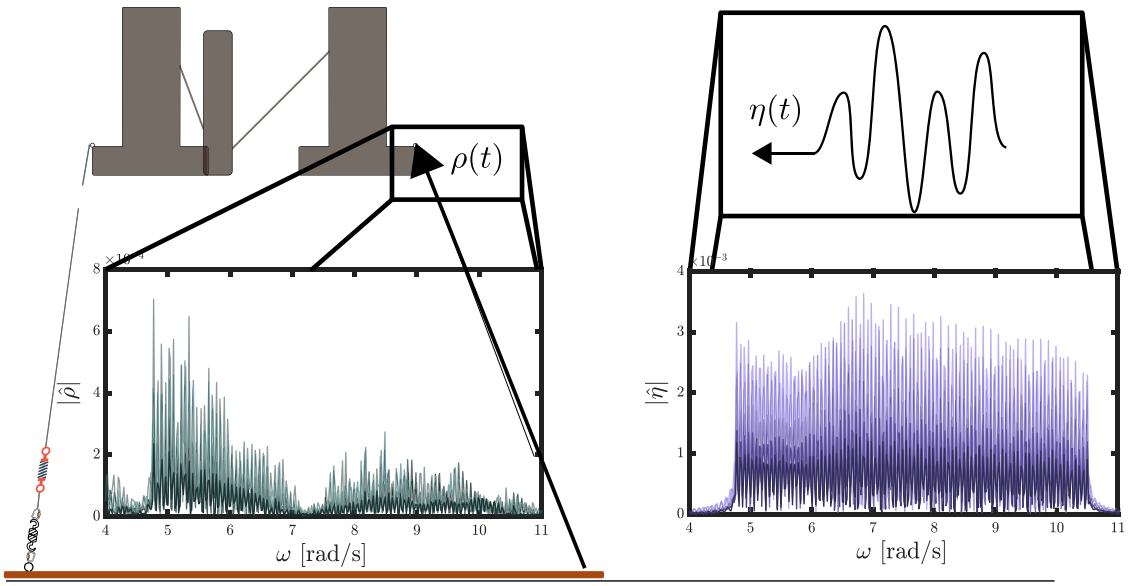


Fig. 17. Frequency-domain amplitudes of the multisine wave excitation conditions and corresponding fairlead radial displacement. The floater dynamics act as a low-pass filter, limiting the effective identification bandwidth.

bandwidth is limited to the frequency range over which the floating structure exhibits a significant dynamic response, thereby reducing the useable identification bandwidth.

This limitation is graphically illustrated in Fig. 17, where the frequency-domain amplitudes of the five multisine excitation conditions are reported together with the corresponding fairlead radial displacement. It can be observed that the floater dynamics effectively act as a low-pass filter, significantly attenuating the response of the fairlead radial coordinate (ρ) at higher frequencies.

Despite this limitation, the multisine conditions were employed as excitation inputs for model synthesis, as they represent the most effective experimental strategy to excite the system over the widest achievable frequency range. Following the procedure outlined in Section 4, the force-to-motion frequency response at the fairlead was constructed by averaging the individual input–output frequency responses obtained from the five multisine tests. The resulting non-parametric model is shown in Fig. 18, where the individual identified transfer functions ($\tilde{G}_{m,l}$) are reported together with their ensemble average, highlighted by the bold black curve.

Given the shape of the identified frequency response, a zero-order transfer function is adopted. From a physical perspective, this behaviour can be directly attributed to the dominance of the axial stiffness, which is expected for taut-leg mooring systems. Accordingly, from Eq. (5), the resulting stiffness is constant, consistently with the spring-based representation adopted in the identification procedure.

The identified constant gain, $\tilde{G}_{m,l} = 30.4$, has units of [N/m] and provides an accurate estimate of the stiffness of the spring employed in the experimental campaign, as reported in Table 4.

5.2. Validation and results

To assess the model performance, the identified model was validated against the extreme wave conditions tested during the experimental campaign. The selected condition corresponds to an irregular wave characterised by a significant wave height $H_s = 86.2$ mm and a peak period $T_p = 1.24$ s. Five independent realisations of this sea state were considered.

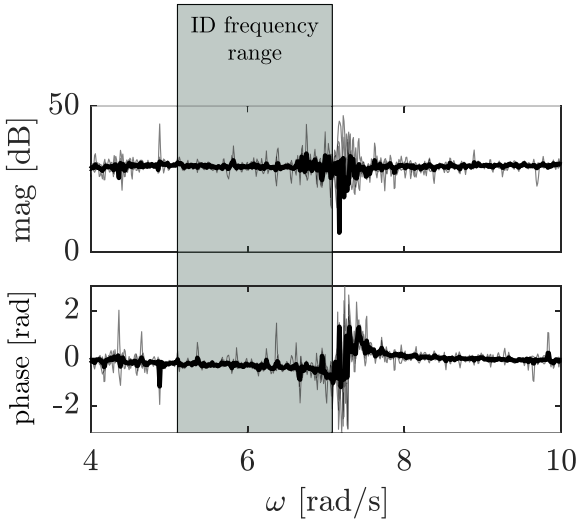


Fig. 18. Non parametric identification of the line model $G_{m,l}$. The bold line represents the average model across the exciting conditions.

The model outputs are reported in Fig. 19. Overall, the three-line mooring model captures the system response well across all tested conditions. Two remarks are worth highlighting.

First, although the adopted accuracy index falls below the threshold value of 0.8, it should be noted that this metric is particularly demanding. Second, the response associated with the first realisation is not reproduced perfectly. However, inspection of the corresponding time histories indicates that the main discrepancy is associated with a small shift in the mean offset. This deviation can reasonably be attributed to several experimental factors, such as stretching of the nylon fibres or slight variations in the water level due to evaporation, which may have a non-negligible impact on offset values at this model scale.

It is important to note that, despite these differences in mean offset, the dynamic behaviour of the system is accurately captured. In particular, the scaled correspondence between the fairlead radial

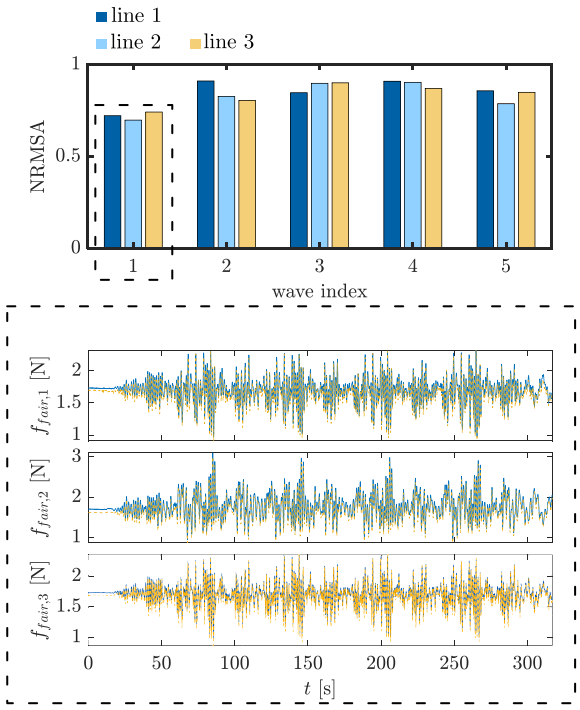


Fig. 19. Time-domain validation of the identified mooring model under extreme irregular wave conditions. Experimental measurements and model predictions are compared for five independent realisations.

displacement and the measured mooring forces is preserved across all cases.

Under this assumption, it would in principle be possible to reconstruct the full six-degree-of-freedom force vector at the centre of gravity. However, such quantities cannot be directly validated experimentally and are therefore not pursued further in this study.

6. Limitations of the proposed identification technique

Within the proposed framework, a linear frequency-domain system identification procedure is adopted. Owing to the constant I/O relationship introduced by the coordinate transformation, the selected linear model structure is deemed sufficient for the considered application. Nevertheless, performing the identification in the frequency domain remains advantageous, as it allows the linear, or locally linearised, response of the mooring system to be captured when more complex operating conditions arise. Although the forces acting at the device CoG are affected by geometric nonlinearities, such effects are effectively accounted for through the adopted change of coordinates.

It is recognised that, even in the case of a spread mooring layout, the proposed approach may encounter limitations in defining a unique and well-posed I/O relationship. In particular, a nonlinear axial stiffness may require the adoption of an explicitly nonlinear model structure. This becomes mandatory when catenary mooring systems are considered, owing to the significant variability associated with line weight distribution and seabed interaction. Furthermore, for catenary layouts, the SISO assumption no longer holds, as the system response is inherently coupled across multiple degrees of freedom. The inclusion of such complex scenarios therefore affects not only the choice of model structure, due to the nonlinear system response, but also the validity of the SISO assumption, since, for instance, current-induced loads may influence the line response in the azimuthal direction φ.

In practical applications, the applicability of any identification model must be assessed in relation to the available measurements. In particular, the absolute motion of the floating structure is generally not directly accessible, and only relative or partial measurements can be obtained. This limitation can be addressed by formulating the identification problem in terms of relative motions or measured responses, or by embedding the identification framework within an observer-based or output-only setting.

An inherent limitation of offline identification techniques should also be acknowledged. This is evident even in relatively simple scenarios, such as the experimental tests presented in Section 5, where variations in draft prevent the accurate identification of the tension offset. Similar issues may arise in real-world applications due to slow time-varying effects influencing the mooring dynamics, including, among others, marine growth (DNV, 2015).

Similar considerations apply to the identification uncertainty associated with the mooring properties themselves. The axial stiffness of taut and semi-taut synthetic lines is known to vary over the service life due to fibre creep and load history (DNV, 2015; Weller et al., 2015), the pretension can drift as a consequence of anchor set-in, hull draft variations, or long-term relaxation of the lines, and the as-built properties of the mooring system may differ from their design values, resulting in a discrepancy between the identified model and the real system. These effects define a natural direction along which the identified model could be probed, complementary to the sensitivity to varying wave conditions that is already exercised through the sixteen sea states considered in Section 4.3.

Finally, the system response under harsh environmental conditions is considered. To highlight the limitations of the adopted modelling approach, an extreme sea state is investigated numerically, leveraging the model developed and validated in Section 4. The selected sea state corresponds to the extreme conditions observed at the Pantelleria test site, as reported in Niosi et al. (2023). It is characterised by a significant wave height of $H_s = 7$ m and a peak period of $T_p = 10$s, with wave direction aligned with the bow of the device (*i.e.*, $Dir = 0°$). A simulation duration of three hours was adopted in accordance with mooring standards (DNV, 2015). Given the link between significant wave height and the associated mean drift force, the mean planar offset increases up to approximately 2 m.

Following the same methodology described in the previous section, the NRMSA values for the fairlead forces under this extreme condition are:

$$\mathrm{NRMSA}_{ext} = [0.44, 0.44, 0.61, 0.61].$$

The symmetry of these values reflects the symmetry of the wave direction with respect to the device. Although these NRMSA values are significantly lower than those obtained for scatter-extrapolated sea states, a more in-depth analysis is necessary to better assess the limitations of the linear modelling technique. By examining the first 2000s of fairlead force responses (Fig. 20), the cause of the relatively low NRMSA values becomes apparent. In the OrcaFlex model, the synthetic mooring lines, responsible for the main restoring forces acting on the vessel, are subject to nonlinear effects, particularly due to their inability to sustain compressive loads. Specifically, the restoring force is generated only when the line is in tension, while in compression, the force in each segment is set to zero. This inherent nonlinearity cannot be captured by a linear transfer function. Finally, it is worth emphasising that the identification methodology proposed in this study goes beyond a simple application of linear transfer functions. Despite the simplified nature of the model, it proves capable of effectively representing mooring dynamics under several wave conditions.

7. Conclusions

The inherently complex problem of depicting mooring systems with representative models is considerably challenging. While traditional numerical models can predict such dynamics with good accuracy, they often face limitations primarily due to the computational cost of traditional simulations. In recent years, several researchers have

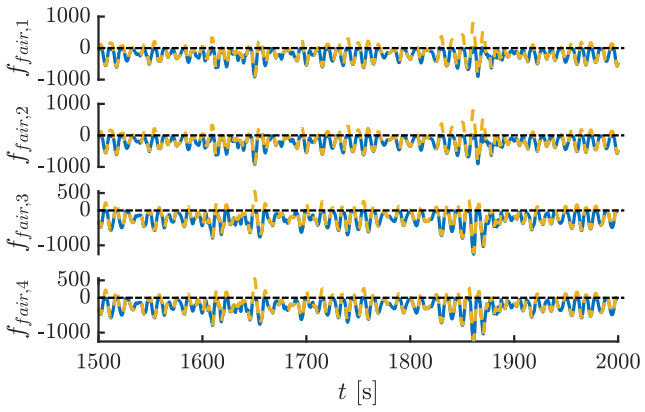


Fig. 20. Fairlead forces (kN) under the extreme wave scenario. Yellow dashed: $\tilde{y}(t)$ (model); blue: $y(t)$ (reference); black dashed: zero baseline.

proposed novel data-based methods to address these issues. The first part of this study provides a review of the state-of-the-art, describing, classifying, and comparing various modelling techniques. Given the limitations of the identified models analysed, and the associated complexity (*e.g.* NNs), we proposed a novel data-based modelling technique based on the ETFE of a single line. This approach emphasises a physically-oriented I/O description and a change in associated coordinates. For a representative case study, the entire mooring problem can be simplified to the definition of an effective and simple mooring model, which can be expressed as a SISO linear model for taut mooring layouts. This mooring modelling technique has been tested and evaluated using a wave energy system as a representative case study, due to its large motions attributed to its resonant nature. The model has demonstrated excellent predictive ability for mooring forces, considering the associated linearity. Given the wide range of exciting conditions, the significant advantages of defining the ETFE are highlighted, which inherently defines a representative set of exciting conditions. Consequently, the associated model is able to function effectively in extrapolation scenarios. Furthermore, the application to an experimental dataset demonstrates the capability of the proposed technique to identify physically meaningful mooring properties in an experimental setting, thereby confirming the practical relevance of the identification approach.

The identification of a single mooring line, while potentially constrained in experimental layouts where bathymetric conditions do not guarantee geometric symmetry, remains appealing due to its intrinsic simplicity and clear physical interpretation.

We conclude by emphasising the necessity of advancing these innovative modelling techniques for mooring systems. This progression towards the definition of representative and computationally efficient models could potentially open up new opportunities for optimisation, providing novel solutions to the complex challenges faced by mooring systems. Furthermore, by leveraging the identified mooring model, the computational cost related to mooring simulations is reduced by three orders of magnitude. This significant reduction exposes the potential, among others, for implementing such methodology in time-consuming algorithms and optimisation techniques.

We finally note that the two case studies presented in this work, comprising a numerical wave energy converter benchmark and the openly available experimental campaign on a 1:96 reduced-scale floating offshore wind turbine of (Niosi et al., 2025), jointly define a reproducible reference case that other identification frameworks can be assessed against, providing an explicit basis for future performance comparisons among system-identification approaches for spread taut and semi-taut mooring systems.

CRediT authorship contribution statement

Bruno Paduano: Writing – review & editing, Writing – original draft, Visualization, Validation, Supervision, Methodology, Investigation, Formal analysis, Data curation, Conceptualization. **Francesco Niosi:** Writing – review & editing, Writing – original draft, Validation, Methodology, Investigation, Conceptualization. **Oronzo Dell'Edera:** Writing – review & editing, Writing – original draft, Validation, Methodology, Investigation. **Davide Issoglio:** Software, Methodology, Investigation, Data curation. **Lorenzo Dutto:** Methodology, Investigation, Formal analysis, Conceptualization. **Nicolás Faedo:** Writing – review & editing, Writing – original draft, Visualization, Investigation, Conceptualization.

Declaration of competing interest

The authors declare that they have no known competing financial interests or personal relationships that could have appeared to influence the work reported in this paper.

Acknowledgements

This study is funded by the Ministry of University and Research (MUR), under Ministerial Decree n. 118 of 2023 (Investment I.4.1 PNRR Public Administration Scholarships), utilising resources from the National Recovery and Resilience Plan (PNRR). The associated Unique Project Code (CUP) is: E14D23001800006. Nicolás Faedo acknowledges the project funded by the European Union - NextGenerationEU under the National Recovery and Resilience Plan (NRRP), Mission 04 Component 2 Investment 3.1 | Project Code: IR0000027 - CUP: B33C22000710006 - iENTRANCE@ENL: Infrastructure for Energy TRAnsition aNd Circular Economy @EuroNanoLab.

References

Allen, J., 1977. Short term spectral analysis, synthesis, and modification by discrete Fourier transform. IEEE Trans. Acoust. Speech Signal Process. 25, 235–238.

Aursand, Mads, Haagensen, Per J, Skallerud, Bjørn H, 2023. Remaining fatigue life assessment of corroded mooring chains using crack growth modelling. Mar. Struct. 90, 103446.

Bjørni, F, Lien, S, Midtgarden, T, Kulia, Geir, Verma, Amrit, Jiang, Zhiyu, 2021. Prediction of dynamic mooring responses of a floating wind turbine using an artificial neural network. IOP Conf. Ser.: Mater. Sci. Eng. 1201, 012023.

Bradshaw, Aaron S., Story, Maeve, Perepelitsa, Irina, Baxter, Christopher D.P., Partovi-Mehr, Nasim, Moaveni, Babak, Hines, Eric M., 2024. A case study of foundation damping in a piled offshore wind jacket structure. Soil Dyn. Earthq. Eng. 180, 108605.

Brommundt, Matthias, Krause, Ludwig, Merz, Karl, Muskulus, Michael, 2012. Mooring system optimization for floating wind turbines using frequency domain analysis. Energy Procedia 24, 289–296, Selected papers from Deep Sea Offshore Wind R&D Conference, Trondheim, Norway, 19-20 January 2012.

Cai, Hongyong, Zhang, De-Qing, Du, Junfeng, Yuan, Zhi-Ming, Jiang, Zhenqiang, 2026. Safety analysis of floating multi-module systems under connector failure. Eng. Struct. 349, 121916.

Carapellese, Fabio, Pasta, Edoardo, Sirigu, Sergej Antonello, Faedo, Nicolás, 2023. SWINGO: Conceptualisation, modelling, and control of a swinging omnidirectional wave energy converter. Mech. Syst. Signal Process. 197, 110356.

Chen, Jialun, Milne, Ian, Taylor, Paul H, Gunawan, David, Zhao, Wenhua, 2023. Forward prediction of surface wave elevations and motions of offshore floating structures using a data-driven model. Ocean Eng. 281, 114680.

Christiansen, Niels H, Voie, Per Erlend Torbergsen, Høgsberg, Jan, 2015. Artificial neural networks for reducing computational effort in active truncated model testing of mooring lines.

Christiansen, Niels, Voie, Per, Høgsberg, Jan, Sødahl, Nils, 2013. Efficient mooring line fatigue analysis using a hybrid method time domain simulation scheme. In: Proceedings of the International Conference on Offshore Mechanics and Arctic Engineering - OMAE, vol. 1.

Chung, Minwoong, Kim, Seungjun, Lee, Kanghyeok, Shin, Do Hyoung, 2020. Detection of damaged mooring line based on deep neural networks. Ocean Eng. 209, 107522.

Corrêa, Fabrício Nogueira, Franz, Alexandra Silva, Pons, Rodrigo Alves, Jacob, Breno Pinheiro, 2023a. Integrity assessment of the mooring lines and risers of floating production systems based on numerical models generated by retroanalysis of measured data: PART II – integrity assessment. Ocean Eng. 273, 113942.

Corrêa, Fabrício Nogueira, Pons, Rodrigo Alves, Albrecht, Carl Horst, Jacob, Breno Pinheiro, 2023b. Integrity assessment of the mooring lines and risers of floating production systems based on numerical models generated by retroanalysis of measured data: PART I – retroanalysis procedure. Ocean Eng. 272, 113910.
Cummins, W.E., 1962. The impulse response function and ship motions. Schiffstechnik 9 (Heft 47, 101–109.
Davidson, J., Giorgi, S., Ringwood, J.V., 2016. Identification of wave energy device models from numerical wave tank data—Part 1: Numerical wave tank identification tests. IEEE Trans. Sustain. Energy 7, 1012–1019.
Davidson, Josh, Ringwood, John V., 2017. Mathematical modelling of mooring systems for wave energy converters - a review. Energies 10.
de Pina, Aloísio Carlos, Albrecht, Carl Horst, de Lima, Beatriz Souza Leite Pires, Jacob, Breno Pinheiro, 2014a. Wavelet network meta-models for the analysis of slender offshore structures. Eng. Struct. 68, 71–84.
de Pina, Aloísio Carlos, de Pina, Aline Aparecida, Albrecht, Carl Horst, de Lima, Beatriz Souza Leite Pires, Jacob, Breno Pinheiro, 2013. ANN-based surrogate models for the analysis of mooring lines and risers. Appl. Ocean Res. 41, 76–86.
de Pina, Aloísio Carlos, da Fonseca Monteiro, Bruno, Albrecht, Carl Horst, de Lima, Beatriz Souza Leite Pires, Jacob, Breno Pinheiro, 2014b. ANN and wavelet network meta-models for the coupled analysis of floating production systems. Appl. Ocean Res. 48, 21–32.
de Pina, Aline Aparecida, da Fonseca Monteiro, Bruno, Albrecht, Carl Horst, de Lima, Beatriz Souza Leite Pires, Jacob, Breno Pinheiro, 2016. Artificial neural networks for the analysis of spread mooring configurations for floating production systems. Appl. Ocean Res. 59, 254–264.
DNV, 2015. DNV-OS-E301 Position mooring. Technical report.
Faltinsen, O., 1993. Sea Loads on Ships and Offshore Structures. Cambridge University Press.
Fathnejat, Hamed, Nava, Vincenzo, 2026. From augmentation to translation: Data generation by conditional hierarchical variational autoencoder, enhancing monitoring mooring systems in floating offshore wind turbines. Eng. Appl. Artif. Intell. 163, 112951.
Fraga, Cláudia Alves Isabel, Neves, 2011. Extreme value distributions. In: Lovric, Miodrag (Ed.), International Encyclopedia of Statistical Science. Springer Berlin Heidelberg, Berlin, Heidelberg, pp. 493–496.
Giorgi, Simone, Davidson, Josh, Ringwood, John V., 2016. Identification of wave energy device models from numerical wave tank data - part 2: Data-based model determination. IEEE Trans. Sustain. Energy 7, 1020–1027.
Gobat, Jason I., Grosenbaugh, Mark A., 2001. A simple model for heave-induced dynamic tension in catenary moorings. Appl. Ocean Res. 23, 159–174.
Guarize, R., Matos, N.A.F., Sagrilo, L.V.S., Lima, E.C.P., 2007. Neural networks in the dynamic response analysis of slender marine structures. Appl. Ocean Res. 29, 191–198.
Hall, M., 2020. Moordyn v2: New capabilities in mooring system components and load cases. In: Proceedings of the International Conference on Offshore Mechanics and Arctic Engineering - OMAE, vol. 9, Export Date: 22 March 2024; Cited By: 8.
Hall, Matthew, Goupee, Andrew, 2015. Validation of a lumped-mass mooring line model with DeepCwind semisubmersible model test data. Ocean Eng. 104, 590–603.
Hersbach, Hans, Bell, Bill, Berrisford, Paul, et al., 2020. The ERA5 global reanalysis. Q. J. R. Meteorol. Soc. 146, 1999–2049.
Hu, Ke, An, Chen, Bai, Xinglan, Su, Jian, Vaz, Murilo A., 2023. Prediction of Chinese-lantern submarine hose tension variation in extreme sea states based on data-driven methods. Appl. Ocean Res. 139, 103687.
Huang, Wei, Chen, Mingsheng, Fan, Tianhui, Guo, Xiangfeng, Liu, Hanyu, Tang, Yichang, 2026. Fully coupled dynamic analysis of a novel modularized wind-aquaculture hybrid platform. Ocean Eng. 348, 124083.
IEC, 2019. IEC TS 62600-30. Technical report.
Ja'e, Idris Ahmed, Ali, Montasir Osman Ahmed, Yenduri, Anurag, Amaechi, Chiemela Victor, Nizamani, Zafarullah, Nakayama, Akihiko, 2022a. Optimization of mooring line design parameters using mooring optimization tool for FPSO (MooOpT4FPSO) with the consideration of integrated design methodology. Ocean Eng. 264, 112499.
Ja'e, Idris Ahmed, Ali, Montasir Osman Ahmed, Yenduri, Anurag, Nizamani, Zafarullah, Nakayama, Akihiko, 2022b. Optimisation of mooring line parameters for offshore floating structures: A review paper. Ocean Eng. 247, 110644.
Jiang, Zhiyu, 2025. Mooring design for floating wind turbines: A review. Renew. Sustain. Energy Rev. 212, 115231.
Kang, Byungho, Park, Semyung, Kwon, Daeyong, 2025. Interpretable prediction of floating offshore wind turbine dynamic responses: An attention-based deep learning approach. Ocean Eng. 335, 121703.
Kendon, Tim, Oritsland, Ola, Baarholm, Rolf, Karlsen, Svein, Stansberg, Carl Trygve, Rossi, Ronaldo, Barreira, Rodrigo, Matos, Vinicius, Sales, Joel, 2008. Ultra-deepwater model testing of a semisubmersible and hybrid verification. In: ASME 2008 27th International Conference on Offshore Mechanics and Arctic Engineering, vol. 4.
Lee, Kanghyeok, Chung, Minwoong, Kim, Seungjun, Shin, Do Hyoung, 2021. Damage detection of catenary mooring line based on recurrent neural networks. Ocean Eng. 227, 108898.
Ljung, Lennart, 1998. System Identification: Theory for the User. Pearson Education.
Ljung, Lennart, 2010. Perspective on system identification. Annu. Rev. Control. 34, 1–12.
Ljung, Lennart, Glover, Keith, 1981. Frequency domain versus time domain methods in system identification. Automatica 17, 71–86.
Ma, Kai-Tung, Luo, Yong, Kwan, Thomas, Wu, Yongyan, 2019. Mooring design. In: Mooring System Engineering for Offshore Structures. Elsevier, pp. 63–83.
Mao, Yixuan, Duan, Menglan, Men, Hongyuan, Zheng, Miaozi, 2025. Local damage identification and nowcasting of mooring system using a noise-robust ConvMamba architecture. Mech. Syst. Signal Process. 224, 112092.
Mao, Yixuan, Wang, Tianqi, Duan, Menglan, 2022. A DNN-based approach to predict dynamic mooring tensions for semi-submersible platform under a mooring line failure condition. Ocean Eng. 266, 112767.
Merigaud, Alexis, 2018. A harmonic balance framework for the numerical simulation of non-linear wave energy converter models in random seas (Ph.D. thesis). Maynooth University, Maynooth, Ireland.
Morison, J.R.R., Johnson, J.W.W., O'Brien, M.P., Brien, M.P.O., 1950. Experimental studies of forces on piles. Coast. Eng. 1, 340–370.
Morison, J.R., O'Brien, M.P., Johnson, J.W., Schaaf, S.A., 1950. The forces exerted by surface waves on pliles. Pet. Trans. AIME. Vol. 189, 149–157.
Mousavi, Zohreh, Varahram, Sina, Ettefagh, Mir Mohammad, Sadeghi, Morteza H, Feng, Wei-Qiang, Bayat, Meysam, 2024. A digital twin-based framework for damage detection of a floating wind turbine structure under various loading conditions based on deep learning approach. Ocean Eng. 292, 116563.
Narayanan, S., Yim, S.C.S., Polo, P.A., 1998. Nonlinear system identification of a Moored structural system. In: The Eighth International Offshore and Polar Engineering Conference.
Niosi, F., Begovic, E., Bertorello, C., Rinauro, B., Sannino, G., Bonfanti, M., Sirigu, S.A., 2023. Experimental validation of orcaflex-based numerical models for the PEWEC device. Ocean Eng. 281, 114963.
Niosi, Francesco, Dell'edera, Oronzo, Glorioso, Mattia, Paduano, Bruno, Giorgi, Giuseppe, Schreier, Sebastian, 2025. Experimental investigation and dataset release of a taut-leg mooring system for a semi-submersible floating offshore wind turbine. Ocean Eng. 328, Cited by: 1; All Open Access, Hybrid Gold Open Access.
Niosi, Francesco, Parrinello, Luca, Paduano, Bruno, Pasta, Edoardo, Carapellese, Fabio, Bracco, Giovanni, 2021. On the influence of mooring in wave energy converters productivity: the PeWEC case. In: 2021 International Conference on Electrical, Computer, Communications and Mechatronics Engineering. ICECCME, pp. 1–6.
Ogilvie, T.F., 1964. Recent progress toward the understanding and prediction of ship motions. In: Proc. of the 5th Symposium on Navan Hydrodynamics, vol. ACR-112, Bergen, pp. 3–79.
Paduano, Bruno, Carapellese, Fabio, Pasta, Edoardo, Bonfanti, Mauro, Sirigu, Sergej, Basile, Dario, Pizzirusso, Domenica, Faedo, Nicolas, Mattiazzo, Giuliana, 2024. Experimental and numerical investigation on the performance of a moored pitching wave energy conversion system. IEEE J. Ocean. Eng..
Paduano, B., Carapellese, F., Pasta, E., Faedo, N., Mattiazzo, G., 2022. Optimal controller tuning for a nonlinear moored wave energy converter via non-parametric frequency-domain techniques. In: Renew.
Paduano, Bruno, Carapellese, Fabio, Pasta, Edoardo, Sergej, Sirigu, Faedo, Nicolas, Mattiazzo, Giuliana, 2023. Data-based control synthesis and performance assessment for moored wave energy conversion systems: the PeWEC case. IEEE Trans. Sustain. Energy.
Paduano, B, Pasta, E, Carapellese, F, Papini, G, Baltazar, J, Faedo, N, Mattiazzo, G, 2023. Control co-design mooring optimisation for wave energy systems: a three-tethered point absorber case. In: IFAC-PapersOnLine. 56, pp. 11717–11722, 22nd IFAC World Congress.
Palm, Johannes, 2017. Mooring dynamics for wave energy applications (Ph.D. thesis). Chalmers University of Technology.
Papini, Guglielmo, Paduano, Bruno, Pasta, Edoardo, Carapellese, Fabio, Mattiazzo, Giuliana, Faedo, Nicolás, 2023. On the influence of mooring systems in optimal predictive control for wave energy converters. Renew. Energy 218, 119242.
Pascoal, R., Huang, S., Barltrop, N., Soares, C. Guedes, 2005. Equivalent force model for the effect of mooring systems on the horizontal motions. Appl. Ocean Res. 27, 165–172.
Pascoal, R., Huang, S., Barltrop, N., Soares, C. Guedes, 2006. Assessment of the effect of mooring systems on the horizontal motions with an equivalent force to model. Ocean Eng. 33, 1644–1668.
Pasta, Edoardo, Faedo, Nicolás, Mattiazzo, Giuliana, Ringwood, John V, 2023. Towards data-driven and data-based control of wave energy systems: Classification, overview, and critical assessment. Renew. Sustain. Energy Rev. 188, 113877.
Peña-Sanchez, Yerai, García-Violini, Demián, Penalba, Markel, Zarketa-Astigarraga, Ander, Ferri, Francesco, Nava, Vincenzo, Ringwood, John V, 2024. Control co-design for wave energy farms: Optimisation of array layout and mooring configuration in a realistic wave climate. Renew. Energy 227, Cited by: 0.
Pintelon, R., Schoukens, J., 2012. System Identification: A Frequency Domain Approach, second ed. Wiley, pp. 1–787.
do Prado, Vinícius Garcia, da Fonseca Monteiro, Bruno, de Lima, Beatriz Souza Leite Pires, Jacob, Breno Pinheiro, 2022. Optimal design of mooring systems for floating production units based on metamodel-assisted differential evolution. Ocean Eng. 266, 112752.
Prawin, J., Rao, A. Rama Mohan, 2017. Nonlinear identification of MDOF systems using Volterra series approximation. Mech. Syst. Signal Process. 84, 58–77.

Qiao, Dongsheng, Li, Peng, Ma, Gang, Qi, Xuliang, Yan, Jun, Ning, Dezhi, Li, Binbin, 2021. Realtime prediction of dynamic mooring lines responses with LSTM neural network model. Ocean Eng. 219, 108368.

Raman, Saraswati, Yim, Solomon, 2003. Parametric identification and sensitive study of a nonlinear Moored structure. In: Proceedings of the Thirteenth (2003) International Offshore and Polar Engineering Conference.

Raman, Saraswati, Yim, Solomon, Palo, Paul, 2005. Nonlinear model for sub and superharmonic motions of a MDOF Moored structure, part 1—System identification. J. Offshore Mech. Arct. Engineering-Transactions the Asme - J OFFSHORE MECH ARCTIC ENG 127.

Saad, A.M., Schopp, F., Barreira, R.A., Santos, I.H.F., Tannuri, E.A., Gomi, E.S., Costa, A.H.R., 2021. Using neural network approaches to detect mooring line failure. IEEE Access 9, 27678–27695.

Saincher, Shaswat, Sriram, V., Stoesser, Thorsten, 2025. Shared moorings for floating offshore renewable energy technologies: A review. Renew. Sustain. Energy Rev. 224, 116064.

Sauder, Thomas, Marelli, Stefano, Larsen, Kjell, Sørensen, Asgeir J., 2018. Active truncation of slender marine structures: Influence of the control system on fidelity. Appl. Ocean Res. 74, 154–169.

Schoukens, Johan, Ljung, Lennart, 2019. Nonlinear system identification: A user-oriented road map. IEEE Control Syst. Mag. 39, 28–99.

Schoukens, J., Pintelon, Rik, Ouderaa, Edwin Van Der, Renneboog, Jean, 1988. Survey of excitation signals for FFT based signal analyzers. IEEE Trans. Instrum. Meas. 37, 342–352.

Sidarta, Erdo, Kyoung, Johyun, O'Sullivan, Jim, Lambrakos, Kostas, 2017. Prediction of Offshore Platform Mooring Line Tensions Using Artificial Neural Network. V001T01A079.

Sidarta, Djoni E., O'Sullivan, Jim, Lim, Ho-Joon, 2018. Damage detection of offshore platform mooring line using artificial neural network. In: ASME 2018 37th International Conference on Ocean, Offshore and Arctic Engineering.

Simoes, M. Godoy, Tiquilloca, J. Leonidas Merma, Morishita, H. Mitio, 2002. Neural-network-based prediction of mooring forces in floating production storage and offloading systems. IEEE Trans. Ind. Appl. 38, 457–466.

Simpkins, A., 2012. System identification: Theory for the user, 2nd edition (ljung, l.; 1999) [on the shelf]. IEEE Robot. Autom. Mag. 19, 95–96.

Sirigu, Sergej A., Fontana, Marco, Paduano, Bruno, 2022. Experimental identification of synthetic ropes stiffness for scaled mooring systems. In: Alessandro, Giuseppe, Quaglia, Vincenzo, Carbone Giuseppe Niola, Gasparetto (Eds.), Advances in Italian Mechanism Science. Springer International Publishing, Cham, pp. 891–899.

Sjöberg, Jonas, Zhang, Qinghua, Ljung, Lennart, Benveniste, Albert, Delyon, Bernard, Glorennec, Pierre-Yves, Hjalmarsson, Håkan, Juditsky, Anatoli, 1995. Nonlinear black-box modeling in system identification: a unified overview. Automatica 31, 1691–1724.

Subbulakshmi, A., Verma, Mohit, 2024. Dynamic response analysis of a semisubmersible floating offshore wind turbine subjected to mooring line failure under normal and extreme environmental conditions. Ocean Eng. 304, 117907.

Tang, Yichang, Chen, Xi, Huang, Guozhen, Chen, Mingsheng, Zhang, Kai, Jiang, Yanlin, Li, Tingqiu, Tao, Tao, Yang, Yi, 2024. Dynamic analysis of multi-module floating photovoltaic platforms with composite mooring system by considering tidal variation and platform configuration. Ocean Eng. 312, 119243.

Tang, Da, Xu, Chuanchuan, Yue, Qianjin, Wu, Wenhua, Shi, Zhongmin, Feng, Jiaguo, 2015. Single point mooring system modal parameter identification based on empirical mode decomposition and time-varying autoregressive model. Appl. Ocean Res. 53, 250–256.

Tsukrov, Igor, Eroshkin, Oleg, Paul, Walter, Celikkol, Barbaros, 2005. Numerical modeling of nonlinear elastic components of mooring systems. IEEE J. Ocean. Eng. 30, 37–46.

Ullah, Zahid, Choi, Dong-Ho, 2024. On the importance of mooring cable dynamics in response analysis of submerged floating tunnel using quasi-static and fully coupled dynamic models. Ocean Eng. 302, 117480.

Wang, Xuefei, Liang, Danni, Li, Mengxiao, Stansby, Peter, zhang, Long, 2023. System identification for modelling M4 wave energy converter. In: Proceedings of the European Wave and Tidal Energy Conference, vol. 15.

Wang, Yutao, Wolgamot, Hugh, Watson, Phillip, Gaudin, Christophe, Zhao, Wenhua, Milne, Ian, 2022. Preliminary investigation of a shared mooring arrangement for a floating offshore wind turbine farm in deep water. In: International Conference on Ocean, Offshore and Arctic Engineering.

Wei, Handi, Xiao, Longfei, Liu, Mingyue, Kou, Yufeng, 2021. Data-driven model and key features based on supervised learning for truncation design of mooring and riser system. Ocean Eng. 224, 108743.

Weller, S.D., Johanning, L., Davies, P., Banfield, S.J., 2015. Synthetic mooring ropes for marine renewable energy applications. Renew. Energy 83, 1268–1278.

World Meteorological Organization, 1988. Guide to Wave Analysis and Forecasting. Secretariat of the World Meteorological Organization.

Yang, Yu, Peng, Tao, Liao, Shijun, 2023. Predicting future mooring line tension of floating structure by machine learning. Ocean Eng. 269, 113470.

Yetkin, Murat, Kim, Yooil, 2019. Time series prediction of mooring line top tension by the NARX and Volterra model. Appl. Ocean Res. 88, 170–186.

Yu, Jun, Cheng, Xiaoming, Xie, Chunmei, Lu, Zhen, Ding, Aibing, Wang, Xuefeng, Zhao, Jing, 2024. Hydrodynamic analysis of three-module semi-submersible platform and its mooring design. Ocean Eng. 310, 118576.

Yuan, Lihao, Chen, Yang, Li, Zhi, 2024. Real-time prediction of mooring tension for semi-submersible platforms. Appl. Ocean Res. 146, 103967.

Zhang, Long, Draycott, Samuel, Stansby, Peter, 2024. System identification and generalisation of elastic mooring line forces on a multi-float wave energy converter platform in steep irregular waves. Mech. Syst. Signal Process..

Zhang, Peng, Li, Wenyuan, Li, Sherwin, Wang, Yang, Xiao, Weidong, 2013. Reliability assessment of photovoltaic power systems: Review of current status and future perspectives. Appl. Energy 104, 822–833.

Zhao, Yuliang, Dong, Sheng, Jiang, Fengyuan, Incecik, Atilla, 2021. Mooring tension prediction based on BP neural network for semi-submersible platform. Ocean Eng. 223, 108714.

Zhao, Yulai, Zhu, Yun-Peng, Han, Qingkai, Liu, Yang, 2023. The evaluation of nonlinear output frequency response functions based on tailored data-driven modelling for rotor condition monitoring. Mech. Syst. Signal Process. 197, 110409.